CSIRO PUBLISHING

Invertebrate Systematics, 2017, **31**, 157–179
http://dx.doi.org/10.1071/IS16023

Systematic revision of *Brachypelma* red-kneed tarantulas (Araneae : Theraphosidae), and the use of DNA barcodes to assist in the identification and conservation of CITES-listed species

Jorge Mendoza[A,B,C] *and Oscar Francke*[B]

[A]Posgrado en Ciencias Biológicas, Universidad Nacional Autónoma de México, Av. Universidad 3000, C.P. 04510, Coyoacán, Distrito Federal, Mexico.
[B]Colección Nacional de Arácnidos, Módulo D planta baja, Departamento de Zoología, Instituto de Biología, Universidad Nacional Autónoma de México, 3er circuito exterior, Apto. Postal 70-153, CP 04510, Ciudad Universitaria, Coyoacán, Distrito Federal, Mexico.
[C]Corresponding author. Email: nomeireth@hotmail.com

Abstract. Mexican red-kneed tarantulas of the genus *Brachypelma* are regarded as some of the most desirable invertebrate pets, and although bred in captivity, they continue to be smuggled out of the wild in large numbers. Species are often difficult to identify based solely on morphology, therefore prompt and accurate identification is required for adequate protection. Thus, we explored the applicability of using COI-based DNA barcoding as a complementary identification tool. *Brachypelma smithi* (F. O. Pickard-Cambridge, 1897) and *Brachypelma hamorii* Tesmongt, Cleton & Verdez, 1997 are redescribed, and their morphological differences defined. *Brachypelma annitha* is proposed as a new synonym of *B. smithi*. The current distribution of red-kneed tarantulas shows that the Balsas River basin may act as a geographical barrier. Morphological and molecular evidence are concordant and together provide robust hypotheses for delimiting Mexican red-kneed tarantula species. DNA barcoding of these tarantulas is further shown to be useful for species-level identification and for potentially preventing black market trade in these spiders. As a Convention on International Trade in Endangered Species (CITES) listing does not protect habitat, or control wildlife management or human interactions with organisms, it is important to support environmental conservation activities to provide an alternative income for local communities and to avoid damage to wildlife populations.

Additional keywords: DNA bar-coding, taxonomy, molecular phylogenetics.

Received 15 March 2016, accepted 16 September 2016, published online 26 April 2017

Introduction

Brachypelma smithi (F. O. Pickard-Cambridge, 1897) is commonly known in the pet trade as the Mexican red-kneed tarantula. Because of its bright colouration, docile behaviour, longevity and hardiness in captivity, it has been shipped out of Mexico in large numbers (Reichling 2003). For example, between 1984 and 1991 a key trader shipped 3000 *B. smithi* into the UK and Europe. Similarly, a company based in Mexico City shipped 200 000 tarantulas into the USA over a 10-year period. The same company also admitted that four out of five commercially exploited colonies in the Colima-Guerrero region, containing 30 000–40 000 individuals each (before exploitation), had been stripped of their populations (Smith 1994). Because of these activities, population sizes have been affected and the species was declared threatened. In September 1985, *B. smithi* was officially placed on Appendix II of the Convention on International Trade in Endangered Species (CITES) (Schultz and Schultz 2009).

Tesmoingt *et al*. (1997*a*, 1997*b*) described two new species of red-kneed tarantulas (*B. annitha* and *B. hamorii*) from Mexico based on highly variable external characters such as the colouration of the legs and carapace. The specimens designated as holotypes were obtained from the pet trade, and therefore no exact type localities were provided. West (2005) suggests that *B. annitha* and *B. hamorii* are merely colour morphs of *B. smithi*. Currently, *B. smithi* is thought to have a disjunct geographical distribution with one population in the state of Colima, extending south-eastwards into Michoacán, and another population along the coast of the state of Guerrero (Locht *et al*. 1999).

Species ‘classification’ allows scientists to determine the relationships between species, and species ‘identification’ allows for determining which specimens have been collected. However, taxonomic identifications are often misdiagnosed due to phenotypic and genetic variability, and lack of diagnostic

features of certain life stages (Hebert *et al*. 2003). Morphology-based identifications of mygalomorph spiders are time-consuming and problematic for several reasons. In many groups, spiders can vary in appearance depending on life cycle and gender. It is difficult to identify juveniles, which are the most abundant individuals at certain times of the year (Greenstone *et al*. 2005; Blagoev *et al*. 2009). Barrett and Hebert (2005) extended DNA barcoding to arachnids and show that it is possible to identify spider fauna using a short fragment of the mitochondrial gene coding for cytochrome *c* oxidase 1 (COI).

The traditional DNA barcode is generated by amplifying a 650-bp segment of the mitochondrial COI gene, usually by PCR (Sun *et al*. 2012), and has been shown to be useful in identifying spider species from around the world (e.g. Barrett and Hebert 2005; Arnedo and Fernández 2007; Longhorn *et al*. 2007; Petersen *et al*. 2007; Blagoev *et al*. 2009; Kuntner and Agnarsson 2011; Hamilton *et al*. 2011, 2014; Hendrixson *et al*. 2013, 2015; Montes de Oca *et al*. 2016; Blagoev *et al*. 2016; Ortíz and Francke 2016). However, a distinction must be recognised between the potential of DNA barcodes for defining or delimiting species and their potential for identifying species. DNA barcodes should be encouraged as a supplement to species description and diagnoses, but should not replace morphological data (Will and Rubinoff 2004; Prendini 2005). Even if debate remains about the characters and criteria for species delimitation, most taxonomists agree that evaluating several lines of evidence within a formalised framework is the most efficient approach to defining robust species hypotheses (Pante *et al*. 2015; Hamilton *et al*. 2016; Ortíz and Francke 2016). For instance, morphological data, geographic distributional data, ecology, behaviour and/or phylogenetically informative molecular markers can be considered concurrently to construct robust taxonomic hypotheses using an integrative decision-making process (e.g. Bond and Stockman 2008; Hamilton *et al*. 2011, 2014, 2016; Hendrixson *et al*. 2013, 2015).

With increased smuggling and difficulties in halting traffickers, the institutions responsible for species wildlife protection in Mexico have joined forces with the academic community to develop a project using DNA barcoding. The goal is to be able to identify species quickly and efficiently. The scientific division of the Federal Police and environmental protection agencies, in collaboration with the Thematic Network Barcode of Life in Mexico (Mexbol), are creating a genetic library to facilitate the identification of animals and plants by using codes made from segments of DNA (BWPM 2014).

In an attempt to resolve known problems in morphology-based taxonomy, a revision was undertaken of all the *Brachypelma* type specimens of species deposited in European collections and of material deposited in the Colección Nacional de Arácnidos in Mexico. This provided the basis to morphologically differentiate red-kneed tarantula species. DNA barcoding techniques were then used to identify *Brachypelma* red-kneed species and their respective delimitations. Parsimony and Bayesian inference analyses were employed for phylogenetic analysis; results were compared with morphology as a strategy for better delimitation of Mexican *Brachypelma* red-kneed species. The present study resolves historical and taxonomic problems within the Mexican red-kneed tarantulas and clarifies geographical distributions. It is hoped that these findings will help create better regulations to protect and conserve these endangered species.

Methods

Morphology

The general descriptive format used in the present study follows Mendoza (2014), with some modifications. All measurements are in millimetres and were taken using an ocular micrometer on a stereomicroscope Nikon SMZ645 (Nikon Instruments Inc., New York, NY) for smaller structures, and a digital caliper with an error of 0.1 mm for larger structures. Leg and palp measurements were taken along the dorsocentral axis of the left side. Description of tarsal scopulae follows Pérez-Miles (1994). Male palpal bulb keel terminology follows Bertani (2000). Description of spermatheca shape follows the general format used with theraphosids (Pérez-Miles 1989; Bertani 2001). In addition, *Brachypelma* species possess a sclerotised area below the spermatheca, the spermatheca baseplate described and named in this study. For comparative purposes, it is necessary to observe the spermatheca in ventral view (in previous publications, the spermatheca is usually drawn or figured from a dorsal view). The spermatheca baseplate is a sclerotised plate located below the base of the spermatheca. It can be completely fused (e.g. genera *Theraphosa* Thorell, 1870 and *Sericopelma* Ausserer, 1875) or medially divided (e.g. genera *Brachypelma* Simon, 1891 and *Phormictopus* Pocock, 1901). The fused baseplate can be as wide as the base of the spermatheca or only a reduced central area, while each side of the divided plate can be narrower than or equal to half of the spermatheca base width.

The photographs in Figs 3–18, 24–36 and 42–49 were taken with a Nikon Coolpix S10 (Nikon Inc., New York, NY) VR digital camera coupled to a stereomicroscope. Descriptions of colours use the standard names of the 267 colour centroids of the NBS/IBCC Colour System (Mundie 1995) to promote standardisation in colour descriptions of live animals. To avoid differences of perception in colouration caused by calibration of the monitor, we extracted the RGB (Red, Green, Blue) code and Pantone colour from photographs using Photoshop CS Live. The eyedropper tool was clicked over the digital image to obtain the RGB colour code in the Set foreground colour, and cross-checked in the colour libraries for the Pantone solid coat. A standard for illumination was deliberately not established, as fluorescent and incandescent lighting provide different colours for the same sample. Habitat and laboratory images were taken with a Canon G12 digital camera. Habitat shots were taken under natural daylight conditions. Laboratory images were taken with a white background and illumination was provided by one fluorescent 30-W light bulb held ~20 cm from the specimen. After the RGB code was obtained, the real colour of the specimen was inferred using the RGB code of colour centroids. The range of each colour centroid as perceived by the human eye is wide enough to account for errors of observation.

Abbreviations used in the text are as follows. Ocular patterns: ALE, anterior lateral eyes; AME, anterior median eyes; PME, posterior median eyes; PLE, posterior lateral eyes. Legs and palpi: d, dorsal; p, prolateral; r, retrolateral; v, ventral; Rap, retrolateral tibial apophysis; Pap, prolateral tibial apophysis; PL, plumose setae. Palpal bulbs: AK, apical keel; PI, prolateral

inferior keel; PS, prolateral superior keel. Chelicerae: CB, cheliceral band. Spermatheca: Bp, spermathecal baseplate. Spinnerets: PMS, posterior median spinnerets; PLS, posterior lateral spinnerets. In species synonymies, we follow the World Spider Catalog (2016): D, described; *t*, transferred; m, male; f, female. Primers: LCO, low cytochrome oxidase; HCO, heavy cytochrome oxidase. Phylogenetics: L, length; Ri, retention index; Ci, consistency index. Institutions: MNHNP, Museum National d'Histoire Naturelle, Paris; NHM, Natural History Museum, London; SNMF, Senckenberg Naturmuseum, Frankfurt; CNAN, Colección Nacional de Arácnidos, México DF; UNAM, Universidad Nacional Autónoma de México, PROFEPA (acronym in Spanish), Federal Environmental Protection Agency.

Taxa

Specimens were collected throughout the known distribution of the genus *Brachypelma* in Mexico with special attention to the type localities (where possible). Material was fixed in 80% ethanol. The third leg on the right side of each spider was stored in 96% ethanol at −20°C. Tissue samples of 26 specimens were used for DNA extraction, representing eight species of *Brachypelma*, including some identified as *B. annitha*, *B. smithi* and *B. hamorii*. Six tissue samples of *B. hamorii*, five of *B. smithi*, three each of *Brachypelma albiceps* Pocock, 1903, *Brachypelma auratum* Schmidt, 1992, *Brachypelma baumgarteni* Smith, 1993 and *Brachypelma boehmei* Schmidt & Klaas, 1993, two of *Brachypelma klaasi* (Schmidt & Krause, 1994) and one of *B. annitha* were used in this study. Additionally, two sequences were retrieved from GenBank to use as outgroups for phylogenetic analyses: *Psalmopoeus cambridgei* Pocock, 1895 [JQ412455.1] and *Eupalaestrus campestratus* (Simon, 1891) [JQ412446.1], both from the same study (Briscoe *et al*. 2013). We obtained sequences of mitochondrial COI from the 26 samples (Appendix 1). Vouchers were deposited in the CNAN and assigned a unique number (CNAN-Ar00xxxx). All sequences were submitted to GenBank, and accession numbers and specimen information are provided in Table 1. For species diagnoses, molecular autapomorphies were obtained with the function *nucDiag* of the R package SPIDER (Brown *et al*. 2012). Diagnostic nucleotides are coded according to their relative position in the alignment (1–641), as defined in Table 2.

DNA protocols

DNA isolation, PCR amplification and sequencing were performed at the Laboratorio de Sistemática Molecular,

Table 1. GenBank accession codes for tissue samples, deposited in the Laboratorio de Sistemática Molecular (Zoología) at the Instituto de Biología, UNAM, Mexico City, from which DNA was extracted and sequenced for phylogenetic analyses of seven species in the genus *Brachypelma* Simon, 1891

Psalmopoeus cambridgei and *Eupalaestrus campestratus* sequences published by Briscoe *et al*. 2013; COI, cytochrome *c* oxidase 1; juv., juvenile; subad., subadult; Un, unsexed

Species	Specimen	Voucher ID	COI
Psalmopoeus cambridgei	1 juv. Un	447_SC_AB	JQ412455
Eupalaestrus campestratus	1 juv. Un	446_SC_AB	JQ412446
Brachypelma albiceps	1 ♂	CNAN-Ar003412	KT995328
Brachypelma albiceps	1 juv. ♀	CNAN-Ar007839	KT995331
Brachypelma albiceps	1 juv. ♀	CNAN-Ar007850	KT995391
Brachypelma auratum	1 ♂	CNAN-Ar003658	KT995348
Brachypelma auratum	1 juv. ♀	CNAN-Ar007136	KT995371
Brachypelma auratum	1 juv. ♀	CNAN-Ar007164	KT995397
Brachypelma baumgarteni	1 ♀	CNAN-Ar007151	KT995332
Brachypelma baumgarteni	1 juv. ♀	CNAN-Ar007161	KT995395
Brachypelma baumgarteni	1 subad. ♂	CNAN-Ar007835	KT995382
Brachypelma boehmei	1 ♀	CNAN-Ar007185	KT995359
Brachypelma boehmei	1 ♀	CNAN-Ar007186	KT995337
Brachypelma boehmei	1 ♂	CNAN-Ar007833	KT995343
Brachypelma hamorii	1 ♂	CNAN-Ar003614	KT995325
Brachypelma hamorii	1 ♂	CNAN-Ar007163	KT995334
Brachypelma hamorii	1 ♂	CNAN-Ar007168	KT995378
Brachypelma hamorii	1 ♂	CNAN-Ar007826	KT995381
Brachypelma hamorii	1 ♂	CNAN-Ar007827	KT995387
Brachypelma hamorii	1 ♂	CNAN-T0900	KT995401
Brachypelma klaasi	1 ♂	CNAN-Ar007160	KT995340
Brachypelma klaasi	1 ♂	CNAN-Ar007162	KT995346
Brachypelma smithi	1 ♀	CNAN-Ar004131	KT995375
Brachypelma smithi	1 juv. ♂	CNAN-Ar007140	KT995380
Brachypelma smithi	1 ♀	CNAN-Ar007143	KT995400
Brachypelma smithi	1 ♀	CNAN-Ar007144	KT995385
Brachypelma smithi	1 ♂	CNAN-Ar007832	KT995374
Brachypelma smithi (annitha)	1 ♀	CNAN-Ar003611	KT995325

Table 2. Mitochondrial cytochrome *c* oxidase 1 (COI) DNA sequence of *Brachypelma smithi* and *Brachypelma hamorii*, showing the nucleotide numbering system (1–641) used to designate molecular autapomorphies for species diagnosis

COI mtDNA (nucleotides 1–641)
Brachypelma smithi CNAN-Ar007144 (KT995385)
CTTCTATGGTGGGAACTGCGATAAGAGTAATTATTCGGGTTGAGTTGGGGCAGGTGGGTAGTTTGTTGGGAGATGATCATTTGTATAATGTG ATTGTGACGGCTCATGCTTTGGTCATGATTTTTTTTATGGTAATGCCTATTTTGATTGGTGGGTTTGGGAATTGGATGTTGCCTTTAATGAT GGGTGCTCCTGATATGGCTTTTCCTCGTATGAATAATTTGAGTTTTTGATTGTTGCCTCCTTCTTTGTTTTTGTTGATTTTGTCGTCGTTGAC TGATGTTGGGGTTGGTGCTGGGTGAACTATTTATCCTCCTTTGTCTTCTTTTGTTGGGCATTCTGGGGGTGGTATGGATTTTGCTATTTTTTC TTTACATTTGGCAGGGGCTTCTTCTATTATGGGGTCTGTAAATTTTATTAGAACTGTTTTGAATATGCGTAGATCTGGAATAACAATAGAG CGGGTTCCGTTGTTTGTGTGGTCTGTTCTTATTACGACTATTTTGTTGTTGTTGTCTTTACCTGTTTTGGCTGGGGCTATTACTATGTCATTG TCTGATCGGAATTTTAATACTTCTTTTTTTGATCCGGCTGGTGGGGGGGAACCCGTTTTG
Brachypelma hamorii CNAN-Ar003614 (KT995325)
CTTCTATAGTAGGAACTGCAATGAGAGTTATTATTCGGGTTGAGTTGGGACAGGTGGGTAGTTTATTGGGGGATGATCATTTATATAATGTT ATTGTGACGGCTCATGCTTTGGTGATAATTTTTTTTATAGTAATGCCCATTTTGATTGGTGGGTTTGGAAATTGAATGTTGCCTTTAATGAT GGGTGCTCCTGATATGGCCTTTCCTCGAATGAATAATTTGAGTTTTTGGTTGTTGCCTCCTTCTTTGTTCTTGTTGATTTTGTCGTCGTTAAC TGATGTTGGAGTTGGTGCTGGATGAACGATTTATCCTCCTTTGTCTTCTTTTGTTGGGCATTCTGGAGGAGGGATGGATTTTGCTATTTTTT CTTTGCATTTGGCTGGAGCTTCTTCTATTATGGGATCTGTAAATTTTATTAGTACCGTTTTGAATATGCGAAGATCGGGAATAACTATGGA ACGGGTTCCTTTGTTTGTGTGGTCTGTTCTTATTACAACTATTTTGTTGTTGTTGTCTCTGCCTGTTTTGGCTGGAGCTATTACTATGTTATT GTCTGATCGTAATTTTAATACTTCTTTTTTTGATCCGGCTGGTGGAAGGGATCCTGTGTTGTTTCAACATTTATTTTG

Instituto de Biología, UNAM. Muscle tissue was extracted from the leg by removing ~20 mg of tissue. Genomic DNA was extracted using the Qiagen DNeasy Tissue Kit (Qiagen Sciences Inc., Maryland, USA), following the manufacturer's protocol. The concentration quality of the extracted DNA was quantified with a spectrophotometer (Nanodrop 2000, Thermo Scientific, Delaware, USA) or visualised via agarose gel electrophoresis. DNA amplification was performed using the PCR for the mtDNA barcoding gene region COI. A single set of primers was used: LCO 1490: 5′-GGTCAACAAATCATAA AGATATTGG-3′, together with HCO 2198: 5′-TAAACTTCAG GGTGACCAAAAAATCA-3′ (Folmer *et al*. 1994). This primer set amplified a 710-bp region of the mitochondrial COI gene.

The PCR reaction (100.8 µL) contained 48 µL of 10× PCR buffer, 24 µL of $MgCl_2$, 7.68 µL of forward and reverse primers, 9.6 µL of dNTPs and 3.84 µL of Taq polymerase, using 1 µL of the DNA template for each sample. The PCR program for COI was as follows: initial denaturation at 94°C for 2 min; 30 cycles of denaturation at 94°C for 1 min, annealing at 48°C for 45 s, elongation at 72°C for 2 min 30 s; followed by 7 min of final elongation at 72°C. LCO 1490 and HCO 2198 primers were used for single-stranded sequencing. The accuracy of sequences was verified by independently amplifying and sequencing the complementary strands of all fragments. Primer sequences were removed and complementary strands of DNA assembled into consensus sequences, edited and checked for quality using Geneious R8 (Kearse *et al*. 2012). If complementary strands disagreed (excluding minor mismatches), the sample was amplified and sequenced again to resolve discrepancies.

DNA sequence alignment and phylogenetic analysis

Static alignments of COI gene fragments were generated with MAFFT online ver. 7 (Katoh *et al*. 2002, 2005). The G-INS-I strategy was selected, which performs a global alignment based on a fast Fourier transform (FFT) approximation (Katoh *et al*. 2002). This method is suitable for large datasets comprising sequences with relatively limited variation in length, i.e. few short gaps (Katoh *et al*. 2005). The scoring matrix for nucleotide sequences was set to $1/PAM_K = 2$, gap opening penalty to 1.53 and offset value to 0.

Parsimony analysis of the DNA sequence alignment (641 bp) was conducted with equal weighting using TNT ver. 1.1 (Goloboff *et al*. 2008), with Sectorial Search using five replications as starting points for each hit, Ratchet (2000 iterations) with drifting (100 cycles) and with fusing (five rounds; dumping fused suboptimal trees to prevent clogging). The maximum number of trees retained in memory was 30 000.

We also carried out Bayesian inference using MrBayes ver. 3.2 (Huelsenbeck and Ronquist 2001; Ronquist and Huelsenbeck 2003). The best-fitting model of sequence evolution was selected using jModelTest ver. 1.0.1 (Posada 2008) in accordance with the Akaike information criterion, on the basis of which a GTR + G + I model was applied. The analysis comprised four Markov chain Monte Carlo models, performed for 10 million generations for all DNA sequence alignments. Trees were sampled every 1000 generations and those sampled before stationarity were discarded as burn-in.

The relative support for each node in the topology obtained by the parsimony analysis was calculated in TNT, using 1000 jack-knife pseudoreplicates with heuristic searches consisting of 1000 random addition sequences, followed by ten iterations of tree bisection-reconnection, retaining one tree per iteration. Posterior probabilities are shown for the Bayesian phylogram obtained by the mitochondrial sequence alignments.

Results

Phylogenetic analysis

An alignment containing 641 bp was produced for the COI dataset. Parsimony analyses of these sequences recovered three most-parsimonious trees. The strict consensus tree (L: 440, Ci: 0.646, Ri: 0.804) recovered the monophyly of both *B. hamorii* and *B. smithi* with high jack-knife support; *B. annitha* was found nested in the *B. smithi* clade (Fig. 1). The tree topology recovered *B. hamorii* as a sister species of the clade

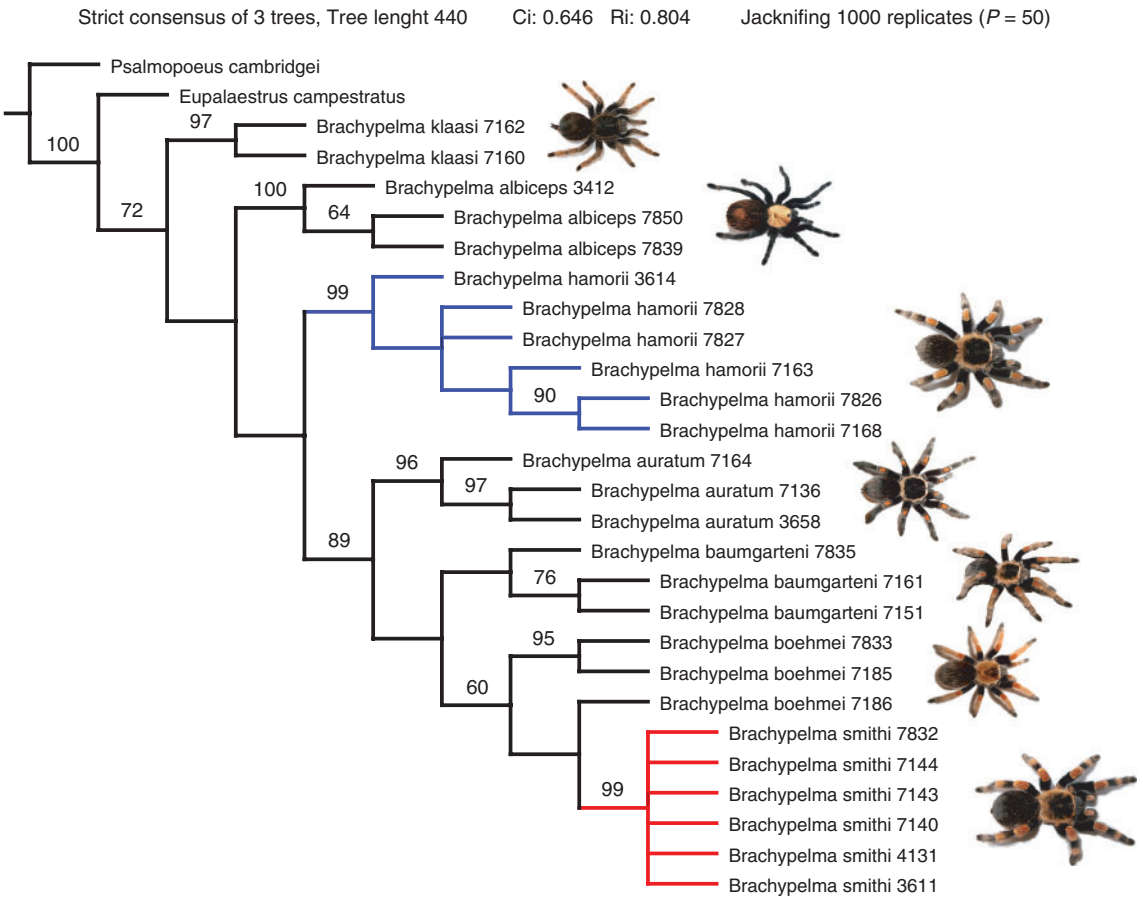

Fig. 1. Strict consensus of the trees obtained by parsimony analysis of 641 aligned nucleotides from barcoding gene cytochrome *c* oxidase 1 (COI) of the mitochondrial genomes of 26 samples from nine *Brachypelma* species, with equal weighting. Jack-knife support with percentages less than 100% indicated above branches.

formed by *B. auratum*, *B. baumgarteni*, *B. boehmei* and *B. smithi*. All *Brachypelma* species analysed except *B. boehmei* were monophyletic, but the interspecific relationships were not as clear, with some nodes lacking support. Despite this, COI has proven useful to identify *Brachypelma* species and is concordant with morphological identification.

Bayesian inference analyses of the COI sequence also recovered the monophyly of both *B. hamorii* and *B. smithi* as separate species, with high posterior probability: 0.996 for the *B. smithi* clade and 1 for *B. hamorii* (Fig. 2). The topology recovered shows *B. hamorii* as a sister species of the clade formed by *B. smithi*, *B. auratum*, *B. baumgarteni* and *B. boehmei*. In this analysis, the three samples available for *B. boehmei* recovered the species as monophyletic. However, no resolution was shown for interspecific relationships in the group comprising *B. boehmei*, *B. baumgarteni* and *B. auratum*.

Despite the differences between the parsimony and Bayesian analyses, *Brachypelma* species can be identified with high accuracy using barcodes. In both cases, *B. hamorii* is the sister species of *B. smithi*, *B. auratum*, *B. baumgarteni* and *B. boehmei*, although the relationships between these species require further resolution.

Taxonomy

Family **THERAPHOSIDAE** Thorell

Subfamily **THERAPHOSINAE** Thorell

Genus ***Brachypelma*** Simon

Brachypelma Simon, 1891: 338.
Type species: Mygale emilia White, 1856, by monotypy.

Diagnosis

Brachypelma differs from all other known theraphosinae genera by having plumose setae on the prolateral face of leg I trochanter and femur and retrolateral face of the palp. Both sexes lack a plumose pad of setae on leg IV femur. Metatarsus IV is 20–35% scopulated distally. All tarsi scopulae are undivided. The femur of leg III is slightly enlarged, but not swollen as in other genera. The male palpal bulb is distally wide and flattened (i.e. spoon-shaped) and comprises prolateral superior and apical keels, and a small or reduced prolateral inferior keel. Females differ by possessing a

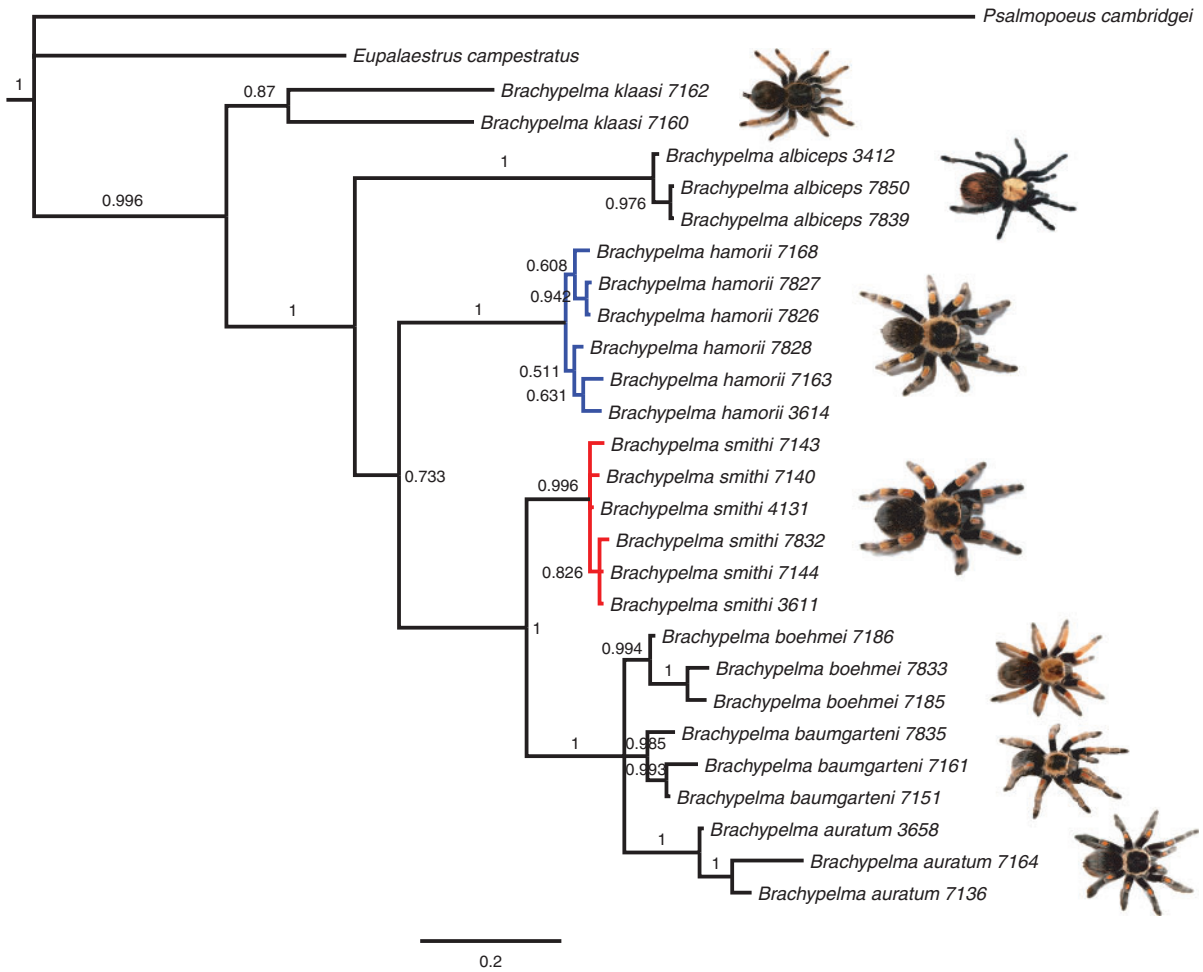

Fig. 2. Bayesian phylogenetic hypothesis of 641 aligned nucleotides from barcoding gene cytochrome *c* oxidase 1 (COI) of the mitochondrial genomes of 26 samples from nine *Brachypelma* species. Posterior probabilities indicated above the branches or close to nodes.

simple undivided/fused spermatheca, apically narrowed. Both sexes possess urticating type I and type III setae; type III located in the dorsoposterior area and type I surrounding these.

Brachypelma smithi (F. O. Pickard-Cambridge)

(Figs 3–23, 42–45, 50, 51, 53–56)

Eurypelma smithi F. O. Pickard-Cambridge, 1897: 20, pl. 1, fig. 4.

Brachypelma smithi (F. O. Pickard-Cambridge, 1897): Pocock, 1903: 103; Locht *et al*., 1999: 198, fig. 5.

Brachypelma annitha Tesmoingt, Cleton & Verdez, 1997*a*: 9, pls 1–6; Tesmoingt *et al*., 1997*b*: 2, pls 7, 8, 11; Peters, 2000: 64, figs 205–207; Peters, 2003: 108, figs 428, 435, 436; Teyssié, 2015: 267, fig. 2. Type locality unknown; species described from pet trade material. The type specimens were never deposited in a museum, according to the authors (M. Tesmoingt and F. Cleton, personal communication) and the MNHNP curator Christine Rollard. Thus, they are presumed to be lost.

Material examined

Holotype. MEXICO: *Guerrero*: juvenile ♂ (labelled as ♀), Dos Arroyos. H. H. Smith (BMNH 1143; also labelled BM1898.12.24.33).

Other material examined. **MEXICO:** *Guerrero*: 1 ♂, 2 ♀, Mpio Acapulco, Dos Arroyos. 13.xii.2013, J. Mendoza (CNAN-Ar007146, CNAN-Ar007143, CNAN-Ar007144); 1 ♂, Mpio Acapulco, 04.i.1965, E. Rivapalacios (CNAN-Ar003086); 1 ♂, Mpio Atoyac, 27.ii.1984, J. G. Julio (CNAN-Ar003434); 1 ♀, Mpio Acapulco, 10.vii.1979, M. Adams (CNAN-Ar003435); 1 ♂, Mpio Acapulco, without additional data (CNAN-Ar003594); 2 ♀, donation received from private collection of J. Mendoza (identified in pet trade as *B. annitha*) (CNAN-Ar004131, CNAN-Ar003611); 3 ♂, Mpio Coyuca de Benítez, 29.viii.2015, J. Mendoza, R. Ramírez (CNAN-Ar010281, CNAN-Ar010275); 1 ♂, 1 ♀, Mpio Acapulco, El Quemado 14.x.2014, A. Ortega (CNAN-Ar007897, CNAN-Ar007896); 1 ♀, Mpio Josue Azueta, 24.viii.2015, D. Ortiz, J. Baldazo (CNAN-Ar007904).

Diagnosis

Brachypelma smithi can be distinguished from all other known *Brachypelma* species (except *B. hamorii*) by the colouration of the carapace and legs: red-orange on the patellae, tibiae and metatarsi, and orange-black starburst striations on the carapace. The shape of the genitalia also differs in both sexes with the palpal bulb being straight and broad, and the spermatheca trapezoidal. It differs from *B. hamorii* by the straight palpal bulb having a broad spoon shape, a wider apical keel and the prolateral superior keel being not as elevated. It also differs in the

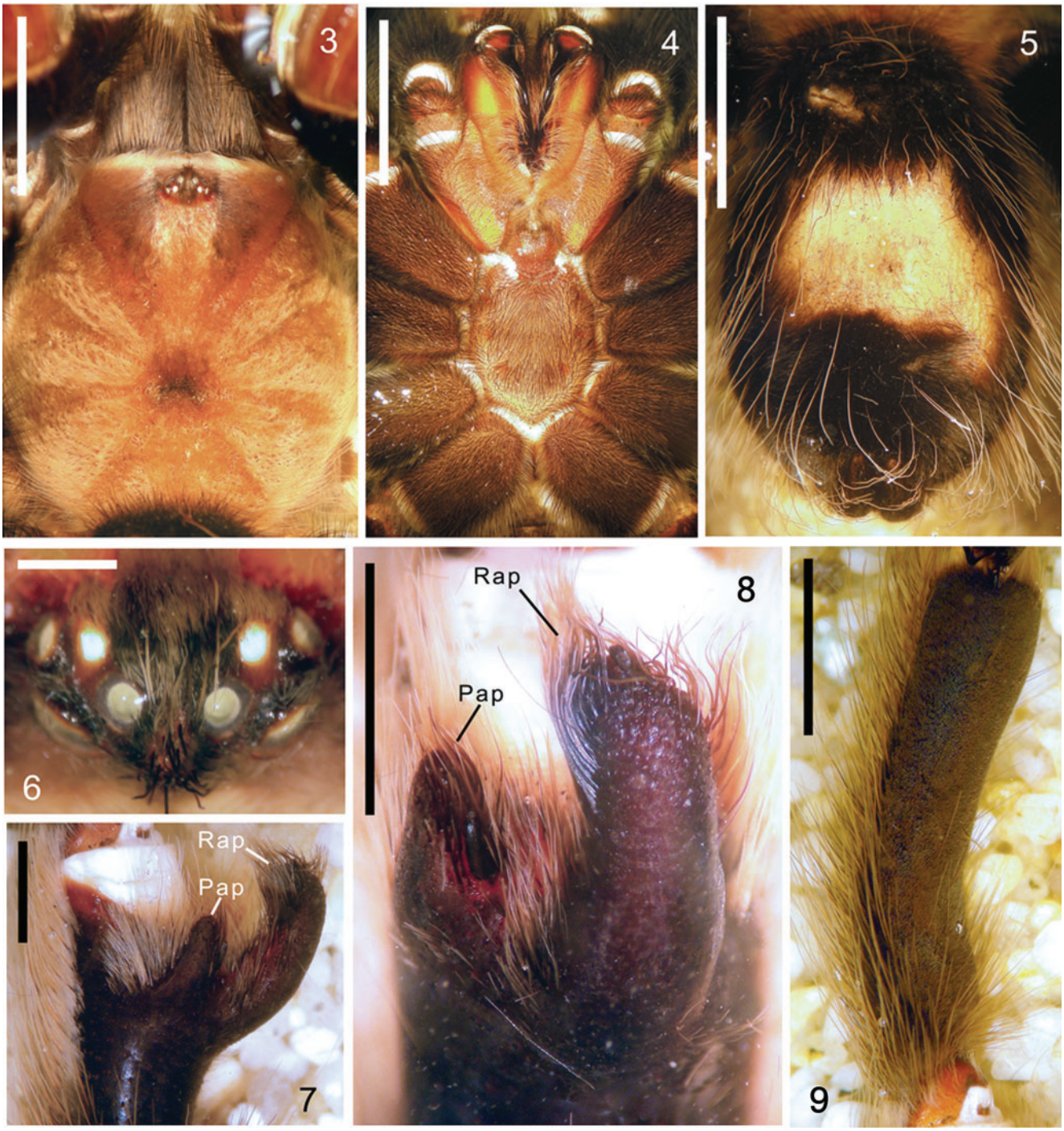

Figs 3–9. *Brachypelma smithi*, male CNAN-Ar007832. *3*, Carapace, dorsal view; *4*, prosoma, ventral view; *5*, opisthosoma, dorsal view; *6*, ocular tubercle, dorsal view; *7*, tibial apophyses, prolateral view; *8*, tibial apophyses, ventral view; *9*, metatarsus I, prolateral view. Scale bars = 10 mm (*3*, *5*), 8 mm (*4*), 5 mm (*9*), 2 mm (*6*, *7*), 1 mm (*8*).

spermatheca with the spermathecal baseplate being divided and subtriangular. The spermathecal ventral face is also striated, while smooth in *B. hamorii*. Although similar in colouration, *B. smithi* differs from *B. hamorii* by the absence of a cheliceral band. Additionally, the patella flame pattern is more colourful than in *B. hamorii*, with brighter orange setae. The lateral setae are yellowish along the length of the legs, while in *B. hamorii* the same are whitish, providing greater contrast with the darker areas.

This species can also be distinguished from other genotyped *Brachypelma* by the following three diagnostic COI nucleotides

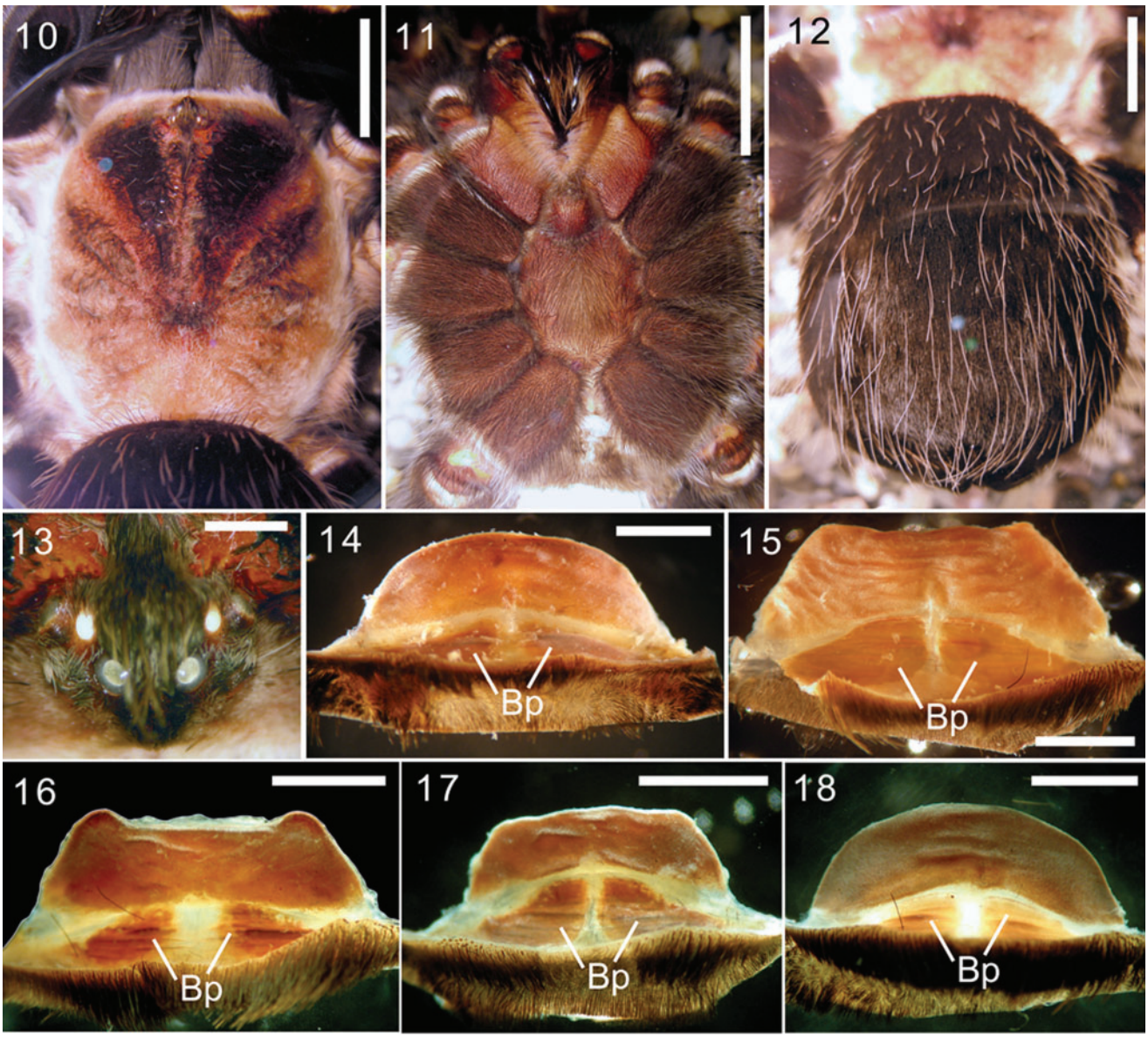

Figs 10–18. *Brachypelma smithi. 10–14* female CNAN-Ar003611. *10*, Carapace, dorsal view; *11*, prosoma, ventral view; *12*, opisthosoma dorsal view; *13*, ocular tubercle, dorsal view; *14*, spermatheca, ventral view; *15–18*, spermatheca ventral view of: *15*, female CNAN-Ar003611; *16*, female CNAN-Ar004131; *17*, female CNAN-Ar007896; *18*, female CNAN-Ar007904. Scale bars = 10 mm (*10–12*), 2 mm (*14–18*), 1 mm (*13*).

($n = 6$): C (116), A (550), A (563). COI p-distances: interspecific above 4%, intraspecific below 1.5%. *Brachypelma smithi* differs from *B. hamorii* by an 8% COI p-distance.

Brachypelma smithi is identified by possessing the following character combination: male palpal bulb with broad spoon-like embolus; prolateral superior keel normally developed, thin and directed retrolaterally; prolateral inferior keel weakly developed, better seen dorsally; and the apical keel strongly developed, wider in the middle (Figs 42–45). Embolus straight and wide along its length, one and a half times longer than the tegulum (Figs 44, 45). Spermatheca semicircular or trapezoidal; ventral face striated. Spermathecal baseplate divided, subtriangular, four times wider than its height (Figs 14–18). Carapace of adult males orange; in females almost black with orange around the border, with black striated pattern and orange around or almost orange with only black caput area. Legs and palpi have dark reddish patellae, while tibiae and metatarsi have yellowish pink colouration distally (see colour pattern) (Figs 19–22, 50, 51, 53–56).

Description

Male (CNAN-Ar007146) (Figs 3–9, 19, 42–45). Body length 46.17 (not including chelicerae and spinnerets). Carapace length 20.18, width 19.50. Caput not markedly elevated; fovea straight, 4.00 wide (Fig. 3). Eyes: anterior eye row procurved,

Figs 19–23. *19–22*, *Brachypelma smithi*, habitus; *23*, habitat. *19*, Male CNAN-Ar007832 in life; *20*, female CNAN-Ar007144 in life; *21*, female CNAN-Ar007901 in life; *22*, female CNAN-Ar007147; *23*, deciduous forest in type locality of *B. smithi*. Photos: J. Mendoza.

posterior eye row recurved. Eye sizes and interocular distances: AME 0.53, ALE 0.77, PME 0.30, PLE 0.53, AME–AME 0.43, AME–ALE 0.17, PME–PME 1.17, PME–PLE 0.20, ALE–PLE 0.33. Ocular tubercle width 2.77, length 2.33; clypeus length 0.27 (Fig. 6). Labium length 2.50, width 3.40, with 72 cuspules. Maxilla inner corner with ~169 (left) and ~166 (right) cuspules. Cheliceral promargin with 8 (left) and 9 (right) teeth (proximal to distal: first to eighth large, first to third large, fourth to sixth medium, seventh large, eighth to ninth small). Sternum length 8.60. Sigillae oval, first, second and third pairs hardly visible, posterior sigilla one and a half times its length from the margin (Fig. 4). Leg formula: IV, I, II, III. Length of legs and palpal segments (femur, patella, tibia, metatarsus, tarsus, total): I 17.18, 9.97, 13.59, 14.21, 9.35, 64.30; II 16.09, 9.16, 12.39, 12.96, 9.07, 59.67; III 14.78, 8.59, 11.66, 14.81, 8.12, 57.96; IV 17.41, 9.11, 14.79, 18.55, 9.84, 69.70. Palp: 11.62, 7.06, 10.12, –, 4.29, 33.09. Spinnerets: PMS 2.07 long, 1.50 apart; PLS 4.00 basal, 2.25 middle, 3.25 distal. Tarsi I–IV entirely scopulated. Metatarsus I densely scopulated, II densely scopulated, III 65% scopulated distally, IV 50% scopulated distally. Tibia I with two tibial apophyses normally developed, which originate from a common base. Prolateral apophysis with one inner conical spine; retrolateral apophysis almost the same width along its length (Figs 7, 8). Metatarsus I curved (Fig. 9). Stridulatory setae: with plumose setae on palp trochanter and femur retrolateral face, leg I trochanter and femur prolateral face. Chaetotaxy (left side): palp femora 1p; patellae none; tibiae I 1p; II 2p, 3v; III 3p, 4v; IV 2p, 3v, 1r; palp 2p, 4v; metatarsi I 2v; II 4v; III 2p, 7v, 2r; IV 1p, 16v. Palp: embolus straight with a broad spoon shape, prolateral superior keel normally developed, thin and directed retrolaterally; prolateral inferior keel weakly developed; apical keel strongly developed, wider in medially; opening of the embolus on the prolateral side, with a concavity just behind the opening that delimits the apical keel boundary from the remaining part of the embolus; embolus apex slightly curved retrolaterally (Figs 42–45). Urticating setae: types I and III arranged in one dorsoposterior patch, black; type III located in an oval dorsomedial area extended towards posterior; type I surrounding the type III area, with intermediates in transition areas between types III and I (Fig. 5). Variations summarised in Table 3.

Colour pattern. In live specimens, adult males with moderate yellowish brown carapace, juveniles and subadults light brown around the border and brownish black dorsomedially; chelicerae dorsally bluish grey; ventral coxae, labium, maxillae and sternum brownish black; abdomen dorsally black with light orange setae, ventrally brownish black. Legs and palpi: femora bluish black, patellae with a proximal dorsomedian dark reddish orange flame-shaped area, distodorsal paramedian light yellowish pink with light orange setae laterally; tibiae proximal half bluish black with light orange setae, distal half pale yellowish pink and metatarsi bluish black with light orange setae and a pinkish white ring at the terminal end; tarsi bluish black (Fig. 19).

Female (CNAN-Ar007143) (Figs 10–18, 20, 51, 53–56). Body length 56.45 (not including chelicerae and spinnerets), carapace length 24.61, width 21.88. Caput not markedly elevated; fovea recurved, 5.00 wide (Fig. 10). Eyes: anterior eye row procurved, posterior eye row recurved. Eye sizes and interocular distances: AME 0.47, ALE 0.72, PME 0.40, PLE 0.52, AME–AME 0.55, AME–ALE 0.30, PME–PME 1.40, PME–PLE 0.17, ALE–PLE 0.52. Ocular tubercle width 3.13, length 2.57; clypeus length 0.53 (Fig. 13). Labium length 3.35, width 4.25, with 88 cuspules. Maxilla inner corner with ~198 (left) and ~207 (right) cuspules. Cheliceral promargin with 8 (left) and 9 (right) teeth (proximal to distal: first to eighth large; first to fifth large, sixth medium, seventh to ninth large). Sternum length 10.6. Sigillae oval; first, second and third pairs hardly visible; posterior sigilla once its length from the margin (Fig. 11). Leg formula: IV, I, II, III. Length of legs and palpal segments (femur, patella, tibia, metatarsus, tarsus, total): I 17.88, 9.95, 13.36, 11.60, 8.22, 61.01; II 15.99, 9.57, 12.09, 12.28, 8.29, 58.22; III 13.74, 9.11, 11.13, 13.60, 8.23, 55.81; IV 17.43, 9.82, 13.40, 16.80, 8.80, 66.25. Palp: 12.45, 7.46, 10.08, –, 8.10, 38.09. Spinnerets: PMS 2.43 long, 2.70 apart; PLS 4.60 basal, 3.10 middle, 4.85 distal. Tarsi I–IV entirely scopulated. Metatarsi I and II entirely scopulated, III 65% scopulated distally, IV 50% scopulated distally. Stridulatory setae: lacking. Plumose setae: on palp

Table 3. *Brachypelma hamorii* and *Brachypelma smithi* variations of some quantitative characters in the specimens' series analysed

Measurements in mm; hyphens represents the interval between the lowest and highest value of each character; when left and right side values were taken it was indicated as (left/right)

Specimen measurements	*Brachypelma hamorii*		*Brachypelma smithi*	
	Males ($n = 13$)	Females ($n = 7$)	Males ($n = 8$)	Females ($n = 7$)
Total length	45.90–51.54	52.57–54.22	44.26–48.40	52.51–58.82
Carapace length	20.50–21.73	22.41–23.81	20.18–21.71	21.06–25.24
Carapace width	19.39–20.44	20.61–21.99	19.47–20.83	19.80–22.55
Sternum length	8.60–9.20	9.80–11.20	8.60–9.10	9.80–10.60
Sternum width	7.90–8.12	9.20–9.30	7.60–7.80	9.20–9.40
Labium length	2.43–2.70	2.67–3.35	2.23–2.50	3.05–3.65
Labium width	2.87–3.70	3.50–4.42	3.10–3.43	3.60–4.45
Chelicaral teeth (left/right)	9–12/10–11	8–9/8–9	8–9/9–10	8–12/8–10
Labial cuspules	109–139	92–132	64–81	88–122
Maxillary cuspules (left/right)	184–203/218–264	277–312/232–272	169–181/155–186	194–265/152–244
Spermatheca length medially	–	1.00–1.25	–	0.97–1.50
Spermatheca base width	–	5.50–6.05	–	4.30–6.30

trochanter and femur retrolateral face, and leg I trochanter and femur prolateral face. Chaetotaxy (left side): femora I 1p, II 1p, palp 1p; patellae palp 1p; tibiae II 2p, 5v; III 3p, 3v; IV 4v; palp 2p, 7v, 1r; metatarsi I 3v; II v; III 1p, 6v, 2r; IV 1p, 16v, 1r. Genitalia: fused semicircular spermatheca with a single receptacle strongly sclerotised, ventral face is faintly striated. Four times wider than its height. Spermatheca baseplate divided, subtriangular, almost as high as half the width of its base, narrowing the upper side towards the outer side (Fig. 14). Variation: semicircular or trapezoidal shape with ventral face very or poorly striated. Baseplate division can vary in length (Figs 15–18). Urticating setae: types I and III arranged in one dorsoposterior patch, black; type III located in an oval dorsomedian area extended to posterior; type I setae surround the area of type III setae with intermediates in transition areas between types III and I (Fig. 12). Variations summarised in Table 3.

Colour pattern. In live specimens, adult females with three carapace patterns: (1) greyish yellowish pink around the border and behind the fovea, with starburst bluish black pattern from fovea to caput (Figs 20, 51); (2) light brown around the border and bluish black in dorsomedian (Figs 22, 50); (3) greyish yellowish pink on almost all of carapace except two longitudinal black patches in the caput (Fig. 21), with juveniles or subadults light brown around the border and brownish black dorsomedially; chelicerae dorsally dark greyish blue; ventral coxae, labium, maxillae and sternum brownish black; abdomen dorsally black with light orange setae, ventrally brownish black. Legs and palpi: femora bluish black, patellae with a proximal dorsomedian area dark reddish orange flame-shaped, distodorsal paramedian area light yellowish pink, with light orange setae laterally; tibiae proximal half bluish black with light orange setae, distal half pale yellowish pink and metatarsi bluish black with light orange setae and a pinkish white ring at the terminal end; tarsi bluish black (Figs 53–56).

Distribution and habitat

Brachypelma smithi is known from the Pacific coast of Guerrero. We indicate on the map three localities from which we were not able to review specimens (La Laja, El Guayabito and Tierra Colorada, specimens were observed by D. Ortiz, J. Hinojosa and V. Jiménez respectively, pers. comm.) (Fig. 61). Burrows occur under large rocks or tree roots in dense thickets or vegetation of dry thorn forests and deciduous forests (Fig. 23). There are no traces of silk at the burrow entrance, and the interior is often multi-tunnelled. The breeding season occurs late in the wet season and early in the dry season (September to January). Egg sacs are constructed in the drier winter months with young emerging and dispersing in late spring, just before the onset of the early summer rains.

Remarks

The type material of *B. smithi* was originally identified as female by F. O. Pickard-Cambridge (1897). Schiapelli and Gerschman inspected the specimen in May 1968 and noticed that it was not a female, but an immature male. Smith (1994) confirmed that the holotype was a juvenile male and redescribed the species using an adult female deposited in the NHM with the code BM1898.12.24.33 and with a male from the Hull-Williams collection without a catalogue number. However, when the material deposited in the NHM was cross-examined for this study, we found that the catalogue number BM1898.12.24.33 was in fact assigned to the holotype and no other specimen was found labelled with that number. The adult male Smith used to redescribe the species could not be located. NHM curator Janet Beccaloni indicated that it was not possible to find any registration for those specimens, and that they are presumably lost. Based on the redescription made by Smith (1994), it is apparent that the specimens he used belong to *B. hamorii* and not *B. smithi*.

Brachypelma hamorii Tesmoingt, Cleton & Verdez

(Figs 24–41, 46–49, 52, 57–60)

Brachypelma hamorii Tesmoingt, Cleton & Verdez, 1997*a*: 9, pls 1–6; Tesmoingt *et al.*, 1997*b*: 3, pls 9–11.

Euathlus smithi (F. O. Pickard-Cambridge, 1897): Baxter, 1993: 73, figs 17, 18, pl. A, figs 1–6 (misidentification).

Brachypelma smithi (F. O. Pickard-Cambridge, 1897): Hancock & Hancock, 1989: 44, fig. 39 (misidentification); Schmidt, 1992*a*: 10; Schmidt, 1992*b*: 14, figs 2, 4; Schmidt, 1993: 82, fig. 190; Smith, 1994: 170, figs 940–956; Tesmoingt *et al.*, 1997*a*: 9, pl. 2, fig. 2 (♀); Tesmoingt *et al.*, 1997*b*: 4, pls 10, 11; Schmidt, 1997: 19, fig. 195; Peters, 2000: 72, figs 235, 236; Peters, 2003: 125, figs 510, 512, 513; Schmidt, 2003: 153, figs 283, 284; Teyssié, 2015: 273, fig. 2 (misidentifications).

Material examined

Neotype. Mexico: *Colima*: ♂, Mpio. Tecoman, 5.xii.2013, D. Barrales, G. Contreras, D. Ortiz (CNAN-T0900).

Other material examined. **Mexico:** *Colima*: 1 ♂, Mpio Tecoman, 1.xii.2012, E. Goyer, E. Hijmensen, D. Ortiz (CNAN-Ar003614); 1 ♀, Mpio Colima, 30.xi.2012, E. Goyer, E. Hijmensen, D. Ortiz (CNAN-Ar004779); 2 ♂, Mpio Tecoman, 5.xii.2013, D. Ortíz, D. Barrales, G. Contreras (CNAN-Ar007163, CNAN-Ar007826); 1 ♂, Mpio Tecoman, 3.xii.2013, D. Ortíz, D. Barrales, G. Contreras (CNAN-Ar007168); 1 ♂, Mpio Manzanillo, iv.2004, IBT (CNAN-Ar010278); 1 ♂, Mpio Manzanillo, 4.xii.2013, D. Ortíz, D. Barrales, G. Contreras (CNAN-Ar010277); 1 ♂, donation received from private collection of J. Mendoza (CNAN-Ar003616); 1 ♂, Mpio 3.xii.2013, D. Ortíz, D. Barrales, G. Contreras (CNAN-Ar007827); 1 ♂, Mpio Manzanillo, 4.xii.2013, D. Ortiz, D. Barrales, G. Contreras (CNAN-Ar007171); 3 ♀, Mpio 11 km SE de Colima (CNAN-Ar007870, CNAN-Ar007872, CNAN-Ar007873); 1 ♀, Mpio. Tecoman, 2.xii.2012, E. Goyer, E. Hijmensen, D. Ortiz (CNAN-Ar007871); *Jalisco*: 2 ♀, Mpio Pihuamo, 30.xi.2012, E. Goyer, E. Hijmensen, D. Ortiz (CNAN-Ar007874, CNAN-Ar010279); 1 ♂, Carretera entre Colima y Jalisco, carretera Colima-Cd. Victoria, 8.viii.2008, A. Cervantes, M. E. Olsen (CNAN-Ar003425); *Michoacán*: 1 ♂, Mpio Lázaro Cardenás, 8.xi.2011, G. Vila (CNAN-Ar003340); 1 ♂, Michoacán, Mpio Aquila, G. Vila (CNAN-Ar003659).

Diagnosis

Brachypelma hamorii can be distinguished from all other known *Brachypelma* species (except *B. smithi*) by the colouration of the legs, with yellow-orange patellae, tibiae and metatarsi; in addition, *B. hamorii* differs in the shape of genitalia in both sexes with palpal bulb curved and short, and spermatheca a rounded trapezoid shape. Differs from *B. smithi* by the narrow curved embolus, the prolateral superior keel being shorter and dorsally wider, and the apical keel being slightly developed. Also, *B. hamorii* differs by the spermatheca ventral face being smooth, and the spermathecal baseplate being elliptic. Although

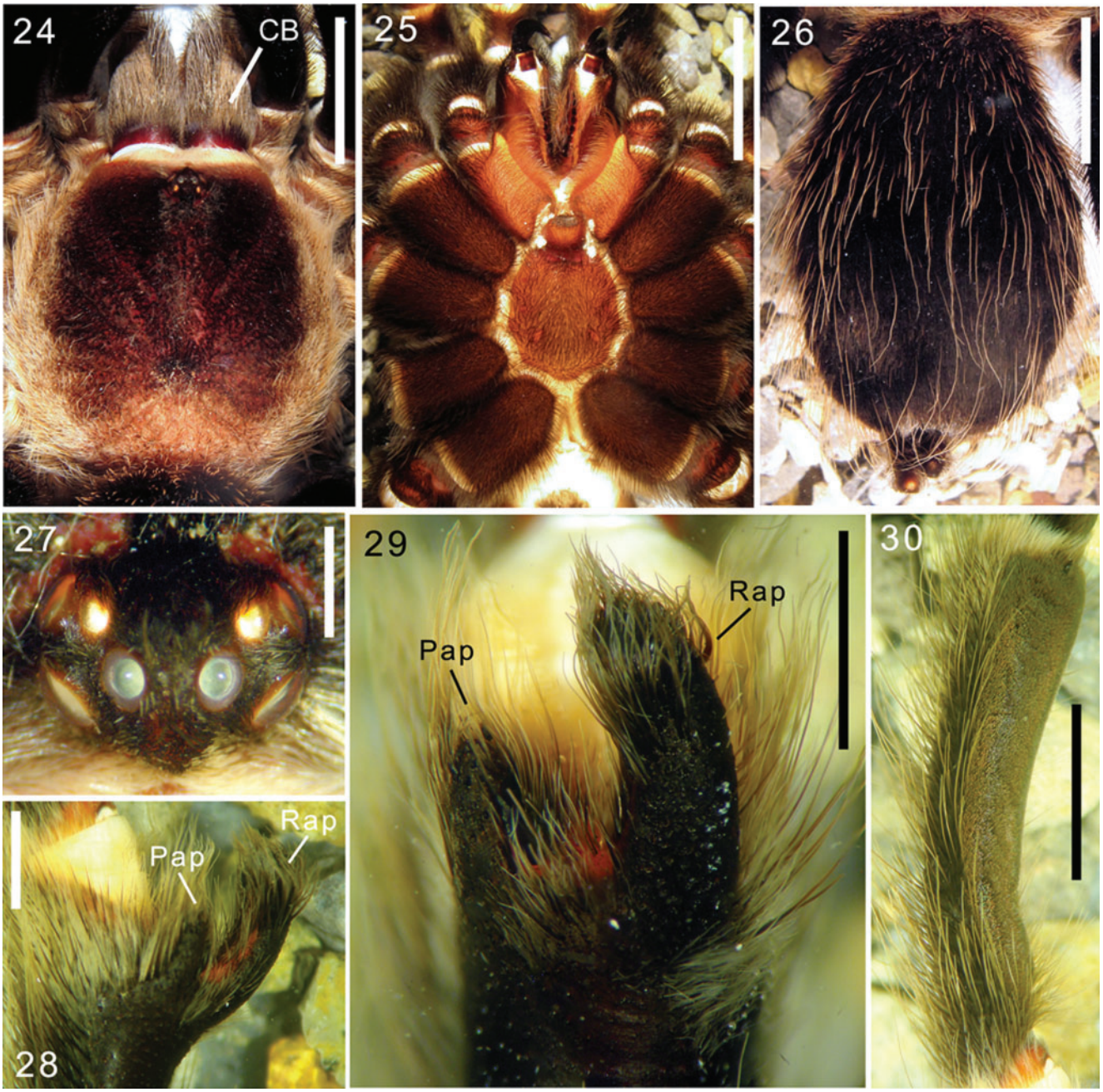

Figs 24–30. *Brachypelma hamorii*, neotype male CNAN-Ar007828. *24*, Carapace, dorsal view; *25*, prosoma, ventral view; *26*, opisthosoma, dorsal view; *27*, ocular tubercle, dorsal view; *28*, tibial apophyses, prolateral view; *29*, tibial apophyses, ventral view; *30*, metatarsus I, prolateral view. Scale bars = 10 mm (*24–26*), 5 mm (*30*), 2 mm (*28*, *29*), 1 mm (*27*).

similar in colouration, *B. hamorii* differs from *B. smithi* by the presence of a cheliceral band (better seen in recently moulted specimens). Patella flame shape not as colourful as in *B. smithi*, with diffuse orange or black setae around the flame-shaped patch. Lateral setae along length of legs whitish, contrasting more with darker areas; the same setae in *B. smithi* are more yellowish. This species can also be distinguished from other genotyped *Brachypelma* by the following eight diagnostic COI nucleotides ($n = 6$): A (11), G (116), C (203), C (254), G (305), A (386), C (425), T (470). COI p-distances: interspecific more than 7.8%, intraspecific less than 0.5%. *Brachypelma hamorii* differs from *B. smithi* by a 7.8–8.0% COI p-distance.

Brachypelma hamorii is identified by the following character combination: male palpal bulb with narrow spoon-like embolus; prolateral superior keel shorter than in other species, thin and directed retrolaterally; prolateral inferior keel weakly developed, directed from dorsal to ventral, better seen dorsally; apical

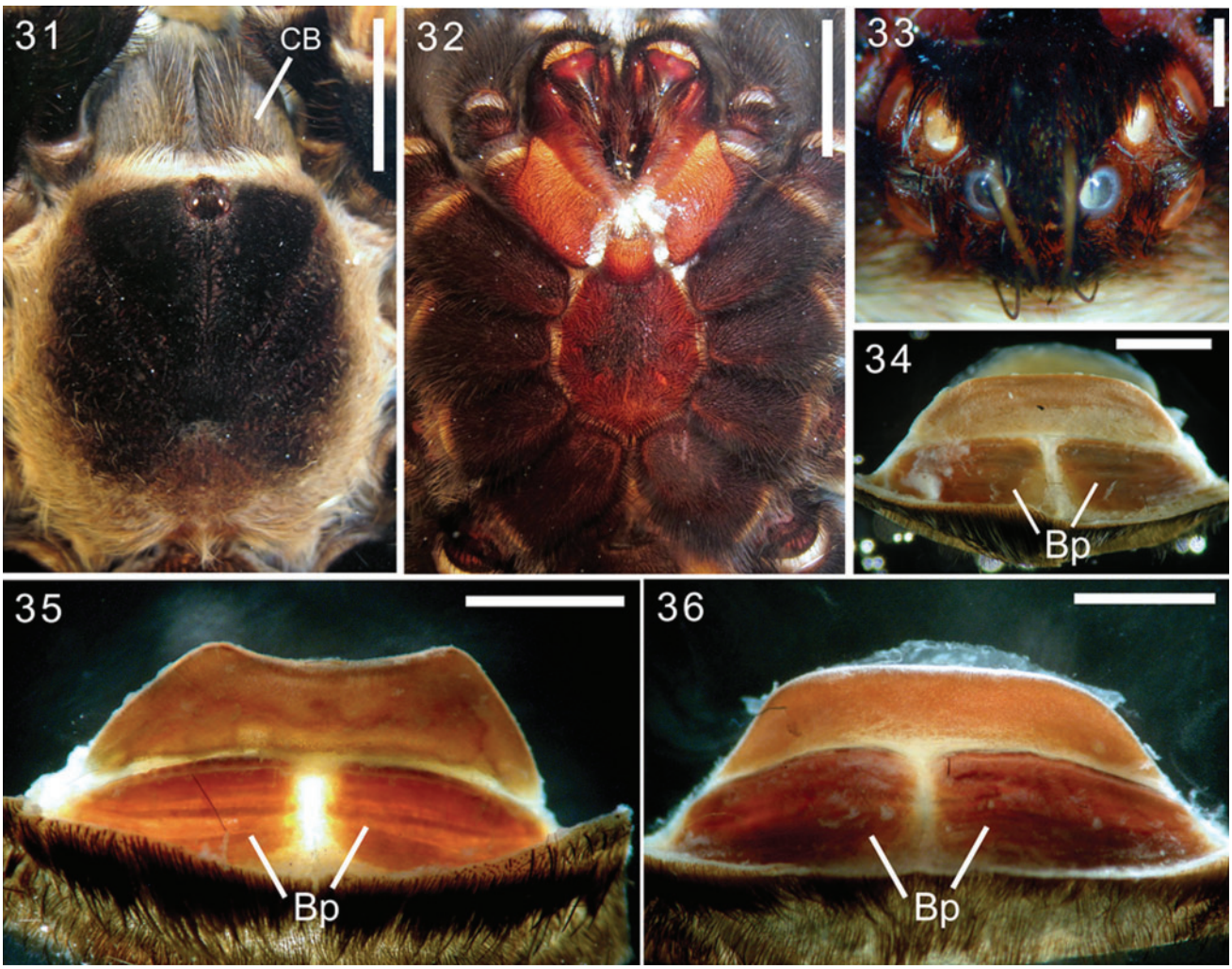

Figs 31–36. *Brachypelma hamorii. 31–34*, Female CNAN-Ar007874. *31*, Carapace, dorsal view; *32*, prosoma, ventral view; *33*, ocular tubercle, dorsal view; *34*, spermatheca, ventral view; *35*, *36* spermatheca ventral view of: *35*, female CNAN-Ar010279; *36*, female CNAN-Ar010280. Scale bars = 10 mm (*31*, *32*), 2 mm (*34–36*), 1 mm (*33*).

keel smaller than in other species, short and thin (Figs 46–49). Embolus tapered along its length, but widening at the apex, and slightly curved dorsally (Figs 48, 49). Spermatheca rounded trapezoid; ventral face almost smooth. Spermathecal baseplate divided, elliptic; five times wider than its height (Figs 34–36). Carapace in general black with orange setae on border, with cheliceral band in most of specimens (see colour pattern for variation). Legs and palpi with deep orange and pale orange on patellae, tibiae and metatarsi with orange yellow/white setae on distal (Figs 37–40, 52, 57–60).

Description

Male (neotype) (CNAN-T0900) (Figs 24–30, 37, 46–49). Body length 51.54 (not including chelicerae and spinnerets), carapace length 21.73, width 20.36. Caput not markedly elevated; fovea recurved, 4.00 wide (Fig. 24). Eyes: anterior eye row procurved, posterior eye row recurved. Eye sizes and interocular distances: AME 0.40, ALE 0.70, PME 0.33, PLE 0.67, AME–AME 0.43, AME–ALE 0.17, PME–PME 1.17, PME–PLE 0.13, ALE–PLE 0.30. Ocular tubercle width 2.47, length 2.20; clypeus length 0.27 (Fig. 27). Labium length 2.63, width 3.40; with 139 cuspules. Maxilla inner corner ~184 (left) and ~218 (right) cuspules. Cheliceral promargin with 9 (left) and 11 (right) teeth (left side, proximal to distal: first to third large, fourth small, fifth to ninth large; right side, first to third large, fourth small, fifth to sixth large, seventh small, eighth to eleventh large). Sternum length 9.20. Sigillae oval; first, second and third pairs hardly visible, posterior sigilla once its own length from the margin (Fig. 25). Leg formula: IV, I, II, III. Length of legs and palpal segments (femur, patella, tibia, metatarsus, tarsus, total): I 19.13, 9.81, 14.72, 15.72, 11.12, 70.50; II 17.45, 9.38, 13.75, 15.21, 9.83, 65.62; III 15.61, 8.85, 12.03, 15.80, 9.46, 61.75; IV 18.93, 9.58, 15.33, 19.13, 11.66, 74.63. Palp: 12.51, 6.92, 11.21, –, 4.66, 35.30. Spinnerets: PMS 2.37 long, 1.67 apart; PLS 4.50 basal, 3.50 middle, 4.15 distal. Tarsi I–IV entirely scopulated. Metatarsi I and II entirely scopulated, III 65% scopulated distally, IV 35% scopulated distally. Tibia I with two tibial apophyses normally

Figs 37–41. *37–40 Brachypelma hamorii*, habitus; *41*, habitat. *37*, Neotype male CNAN-Ar007828, in life; *38*, female CNAN-Ar007874, in life; *39*, female, in habitat (Colima); *40*, female, in habitat (Michoacán); *41*, deciduous forest in Colima, habitat of *B. hamorii*. Photos: J. Mendoza (*37*, *38*), E. Goyer (*39*, *41*), G. Vila (*40*).

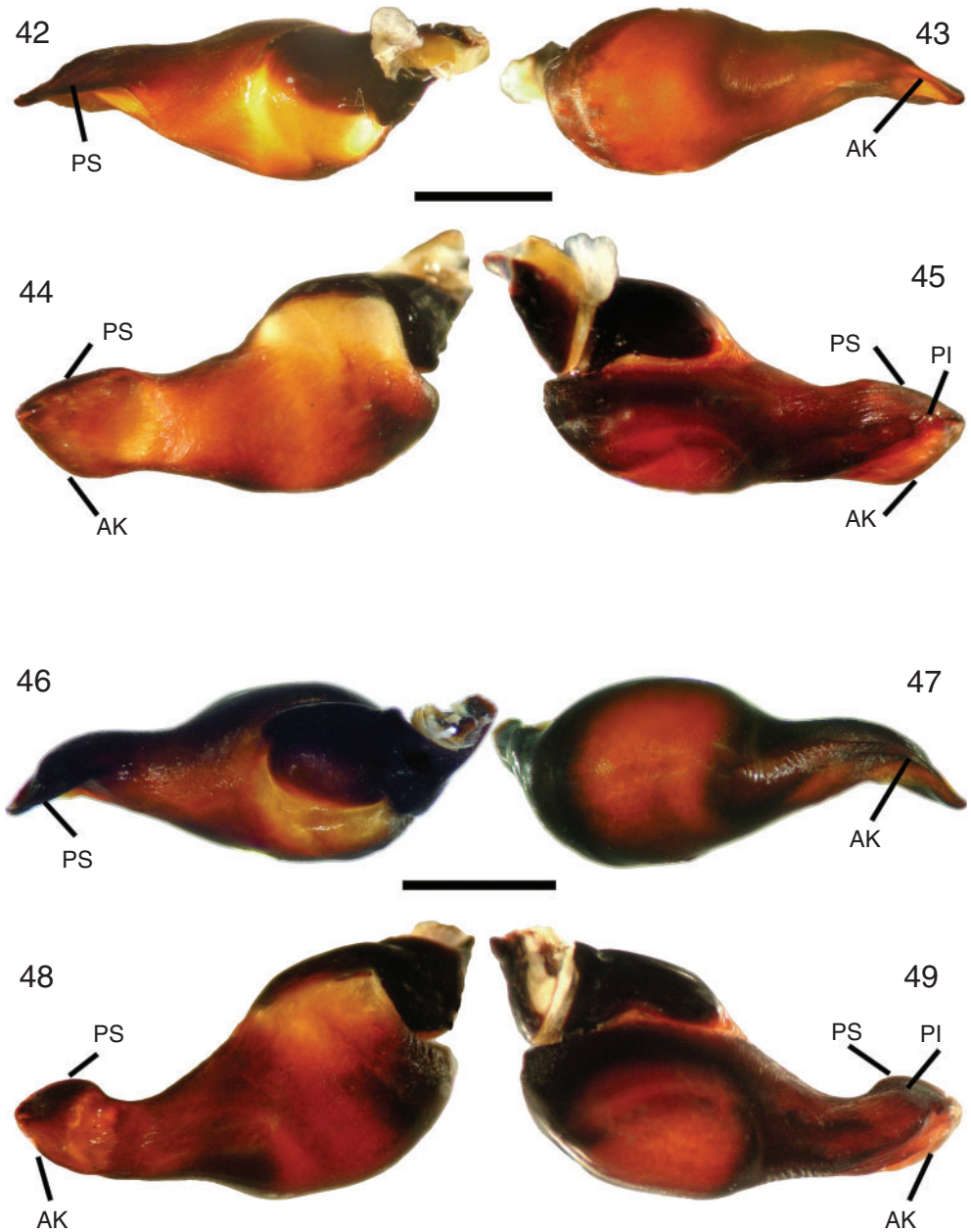

Figs 42–49. *42–45 Brachypelma smithi*, male CNAN-Ar007832; *46–49 Brachypelma hamorii*, neotype male CNAN-Ar007828. Left palpal bulb: *42*, *46*, dorsal view; *43*, *47*, ventral view; *44*, *48*, retrolateral view; *45*, *49*, prolateral view. Scale bar = 2 mm.

developed that originate from a common base. Prolateral apophysis with inner spine half its length; retrolateral apophysis same width along its length, apex slightly curved to prolateral (Figs 28, 29). Metatarsus I curved (Fig. 30). Stridulatory setae: with plumose setae on palp trochanter and femur retrolateral face, and leg I trochanter and femur prolateral face. Chaetotaxy (left side): femora I 1p; palp 1p; patellae none; tibiae I 1p; II 1p, 3v; III 2p, 3v, 1r; IV 2p, 3v, 1r; palp 3p, 1v; metatarsi II 1p, 4v; III 2p, 7v, 1r; IV 9v.

Palp. Embolus with narrow spoon-like shape, slightly curved to dorsal, prolateral superior keel short, thin and directed retrolaterally, prolateral inferior keel weakly developed directed from dorsal to ventral, better seen dorsally, apical keel short and thin. Opening of the embolus on the prolateral side, a concavity located just behind the opening delimits the apical keel boundary from the rest of the embolus. Embolus apex strongly curved towards the retrolateral (Figs 46–49). Urticating setae: types I and III arranged in one dorsoposterior patch, black. Type III located in an oval dorsomedian area extended to posterior; type I setae surround the area of type III setae with intermediates in transition areas between type III and I (Fig. 26). Variations summarised in Table 3.

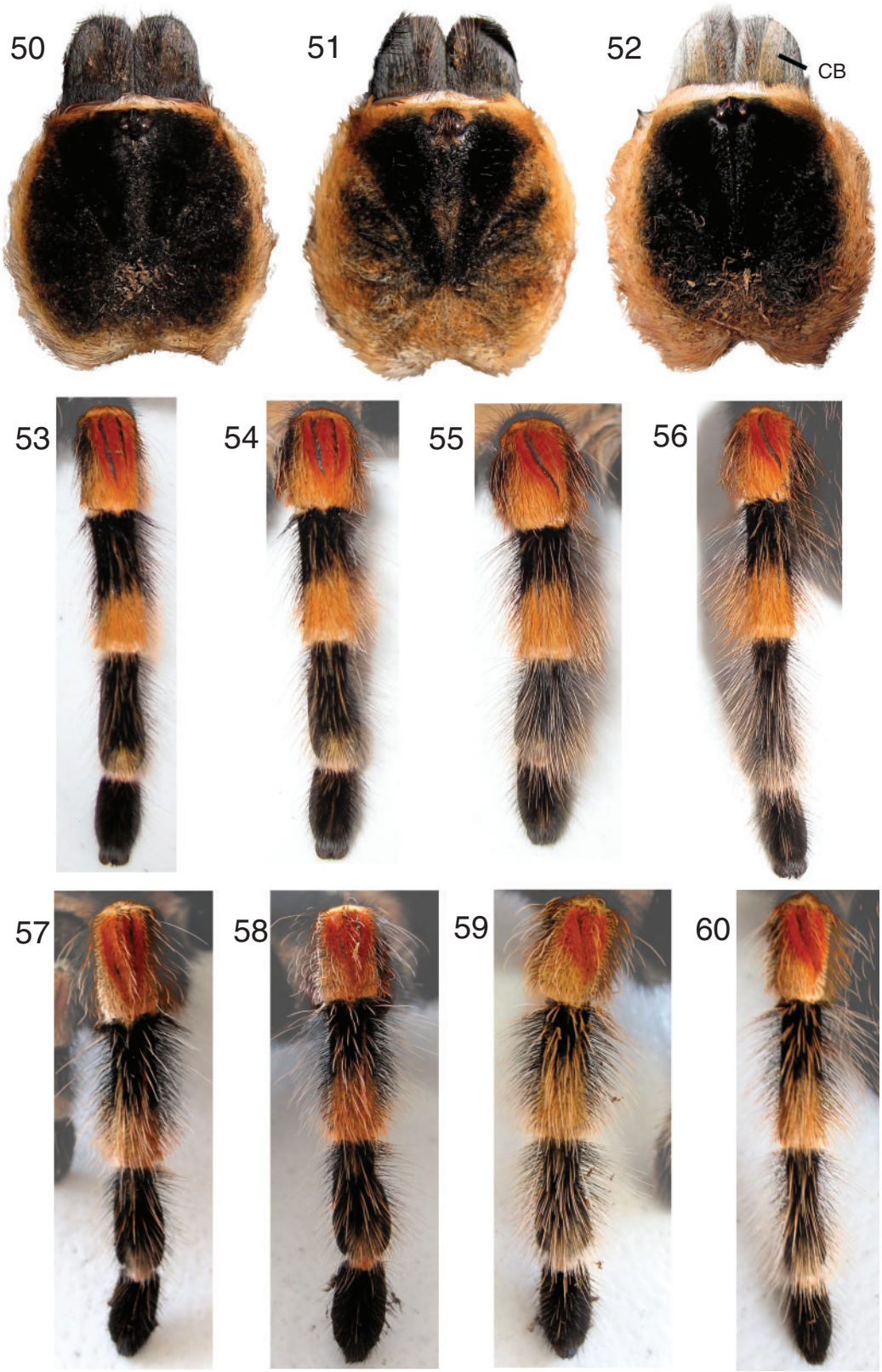

Figs 50–60. *Brachypelma smithi. 50*, female (CNAN-Ar007147) carapace; *51*, female (CNAN-Ar007143) carapace; female (CNAN-Ar007144). *53*, Leg I; *54*, leg II; *55*, leg III; *56*, leg IV; *Brachypelma hamorii.* Female (CNAN-Ar007874). *52*, Carapace; *57*, leg I; *58*, leg II; *59*, leg III; *60*, leg IV.

Colour pattern. In live specimens, adult males with carapace light greyish red around the border and behind the fovea, reddish black from the fovea to caput; chelicerae dorsally brownish pink; ventral coxae, labium, maxillae and sternum brownish black; abdomen dorsally black with light greyish yellowish brown setae, ventrally brownish black. Legs and palpi: femora black, patellae with a proximal flame-shaped dorsomedian area deep orange, distodorsal paramedian area pale orange yellow, with brownish pink setae laterally; tibiae proximal half reddish black with brownish pink setae, distal half pale orange-yellow with brownish pink setae and metatarsi reddish black with brownish pink setae and a yellowish white ring at the terminal end; tarsi black (Fig. 37).

Female (CNAN-Ar007874) (Figs 31–34, 38, 52, 57–60). Body length 53.70 (not including chelicerae and spinnerets), carapace length 23.81, width 21.78. Caput not markedly elevated; fovea straight, 5.00 wide (Fig. 31). Eyes: anterior eye row procurved, posterior eye row recurved. Eye sizes and interocular distances: AME 0.47; ALE 0.67; PME 0.47; PLE 0.70; AME–AME 0.63; AME–ALE 0.37; PME–PME 1.40; PME–PLE 0.20; ALE–PLE 0.33. Ocular tubercle width 2.83, length 2.33; clypeus length 0.50 (Fig. 33). Labium length 3.35, width 4.35 with 92 cuspules. Maxilla inner corner with ~241 (left) and ~277 (right) cuspules. Cheliceral promargin with 8 (left) and 8 (right) teeth (proximal to distal: first to seventh medium, seventh large, eighth medium; first medium, second to third large, fourth to eighth medium). Sternum length 11.20. Sigillae oval, second and third pairs hardly visible; posterior sigilla one and half its length from the margin (Fig. 32). Leg formula: IV, I, III, II. Length of legs and palpal segments (femur, patella, tibia, metatarsus, tarsus, total): I: 16.65, 10.39, 13.22, 12.42, 8.32, 61.00; II: 14.88, 9.42, 11.07, 11.35, 8.50, 55.22; III: 14.09, 8.81, 11.17, 12.41, 8.50, 54.98; IV: 17.28, 9.64, 13.55, 17.23, 9.43, 67.13; palp: 12.40, 7.63, 8.72, – 10.02, 38.77. Spinnerets: PMS, 2.37 long, 2.17 apart; PLS, 5.25 basal, 3.00 middle, 4.60 distal. Tarsi I–IV entirely scopulated. Metatarsi I and II entirely scopulated, III 65% scopulated distally, IV 50% scopulated distally. Stridulatory setae lacking; plumose setae on palp trochanter and femur retrolateral face, and leg I trochanter and femur prolateral face. Chaetotaxy (left side): femora palp 1p; patellae palp 1p; tibiae I 1p; II 2p, 2v; III 3p, 6v; IV 3v; metatarsi I 2v; II 2v; III 2p, 4v, 2r; IV 1p, 8v, 2r. Genitalia: fused rounded trapezoid spermatheca with a single strongly sclerotized receptacle, ventral face almost smooth, five times wider than its height. Spermatheca baseplate divided, elliptic, as high as half the width of its base, outer side slightly smaller than inner (Fig. 34). Variation: semicircular or trapezoidal shape with an incurvature in the upper edge. Ventral face smooth. Baseplate division can vary in length (Figs 35, 36). Urticating setae: types I and III arranged in one dorsoposterior patch, black; type III located in an oval dorsomedian area extended towards posterior; type I surrounding area of type III, with intermediates in transition areas between types III and I. Variations summarised in Table 3.

Colour pattern. In live specimens, adult females with two carapace patterns: (1) brownish pink around the border and black dorsomedially, juveniles and subadults same pattern (Figs 38, 39); (2) pale orange-yellow around the border and behind the fovea, with starburst black pattern from fovea to caput (Fig. 40); chelicerae dorsally light bluish grey with two brownish pink cheliceral bands (not all specimens have clearly visible bands, more readily seen in recently moulted specimens) (Fig. 52); ventral coxae, labium, maxillae and sternum brownish black; abdomen dorsally black with light reddish brown setae, ventrally brownish black. Legs and palpi: femora black, patellae with a proximal dorsomedian deep orange flame-shaped area, distodorsal paramedian area pale orange-yellow (specimens of some populations only present pale orange-yellow on distal half of patella) with brownish pink setae laterally; tibiae proximal half black with brownish pink setae, distal half light orange-yellow with brownish pink setae and metatarsi black with brownish pink setae and a yellowish white ring at the terminal end; tarsi black with a few dorsal brownish pink setae (Figs 57–60).

Distribution and habitat

Brachypelma hamorii is known from the southern Mexican states of Colima, southern Jalisco and the north-western coast of Michoacán (Fig. 61), where it occurs in thorn and deciduous secondary forests (Fig. 41). It is a fossorial species whose modified or self-excavated burrows can be found under fallen logs, large rocks and large tree roots among thorny brush or tall grass thickets. Burrows do not have any silk around the entrance.

Remarks

The type locality of *B. hamorii* is unknown, and the species was described from pet trade material (Tesmoingt *et al*. 1997*a*). The type specimens were never deposited in a museum and, according to the authors (pers. comm.), and to MNHNP curator Christine Rollard, they are lost. Because of the taxonomic confusion between *B. hamorii* and *B. smithi* and the absence of comparative material, we hereby designate a male neotype (CNAN-T0900) to clarify the taxonomic status of *B. hamorii*. Based on our evidence and key features such as the male palpal bulb, this specimen matches the original description of the species.

Schmidt (1992*b*) was the first to notice differences in the morphological features of the male and female sexual organs of what he thought was *B. smithi*. However, due to the lack of information about the precise collection sites of the specimens he had at hand, he mistakenly described the male bulb and spermatheca of another species as those of *B. smithi*, triggering a cascade of subsequent errors. We believe that authors such as Smith (1994), Tesmoingt *et al*. (1997*a*, 1997*b*), Peters (2000, 2003), Schmidt (1992*a*, 1993, 1997, 2003) and Teyssié (2015) incorrectly identified *B. hamorii* specimens as belonging to *B. smithi*.

Discussion

West (2005) mentioned having seen many colour and dorsal pattern variations in *B. smithi*, and considered that *B. annitha* and *B. hamorii* were described based on superficial characters. He also stressed the need for more careful and professional taxonomic studies to solve the question of variants versus what constitutes a valid species in *Brachypelma*.

Tesmoingt *et al*. (1997*b*), in their description of the male palpal bulbs of *B. annitha* and *B. hamorii*, made it possible to readily identify the red-knee tarantula they had determined as *B. smithi*.

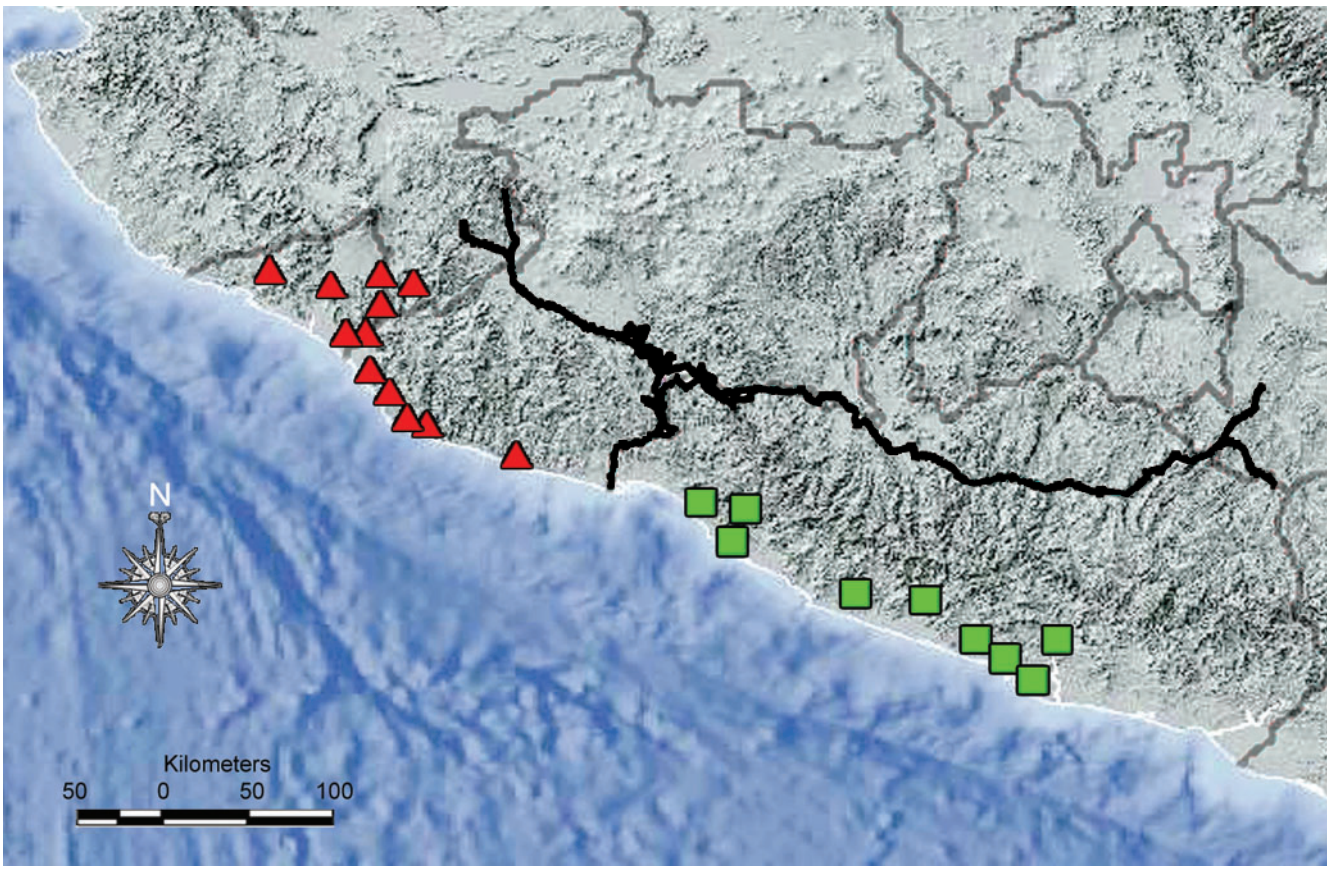

Fig. 61. Map showing records of *Brachypelma* Mexican red-knee tarantulas in Colima, Guerrero and Michoacán states. Triangles, *B. hamorii*; squares, *B. smithi*. The dark black line represents the Balsas River basin.

According to this description, the male palpal bulb of *B. smithi* is curved and tapers towards the embolus. They also mentioned that the shapes of the bulbs of *B. smithi* and *B. hamorii* are fairly similar and without notable morphological distinguishing features. This description fits perfectly with specimens from Colima and Michoacán, but not with those from Guerrero, especially those from the type locality of *B. smithi.* It is thus apparent that *B. smithi* was misidentified and therefore incorrectly referred to. Notwithstanding, the description of *B. annitha* mentions that the male palpal bulb is essentially straight, composed of a pear-shaped bulb narrowing slightly above (or past) the embolus. This consists of a much larger bowl-shaped embolus than in what Tesmoingt *et al*. (1997*b*) incorrectly considered to be *B. smithi*. In summary, their description of the male copulatory apparatus of *B. annitha* matches that of the true *B. smithi* from Guerrero. Therefore, our results confirm that the red-knee tarantulas from Guerrero are *B. smithi*, and that *B. annitha* is the same species, which therefore becomes a junior synonym of *B. smithi*. It is also clear that the populations from Jalisco, Colima and Michoacán are *B. hamorii*.

The geographic distribution of *B. smithi* was previously thought to be disjunct by Smith (1994) and Locht *et al*. (1999). Two main populations were reported: one in Colima and Michoacán and the other in Guerrero. Due to similar colouration between specimens from Colima and Michoacán and those from Guerrero, it was assumed that they belonged to the same species. However, these two populations do not come into contact for two distinct reasons: the Balsas River basin (Fig. 61) acts as a geographical barrier separating the species, and populations of *B. baumgarteni* and *B. boehmei* are found between these two areas (Fig. 62). Our phylogenetic analysis utilising mtDNA proved to be a highly useful complement to morphological data and was able to reliably identify *Brachypelma* species. However, the observed phylogenetic relationships and clades may change with the inclusion of nuclear data.

DNA barcoding

Morphological identification of organisms requires experienced taxonomists. Incomplete identification often occurs when important morphological features are damaged as a result of improper specimen handling (Chan *et al*. 2014). Molecular markers, such as COI, may provide species boundary information in certain taxonomic groups and consequently have the potential to be a rapid and efficient means to delineate and identify species (e.g. Chen *et al*. 2011; Hamilton *et al*. 2014). Unfortunately, molecular identification of species is fraught with the same constraints and inconsistencies that plague

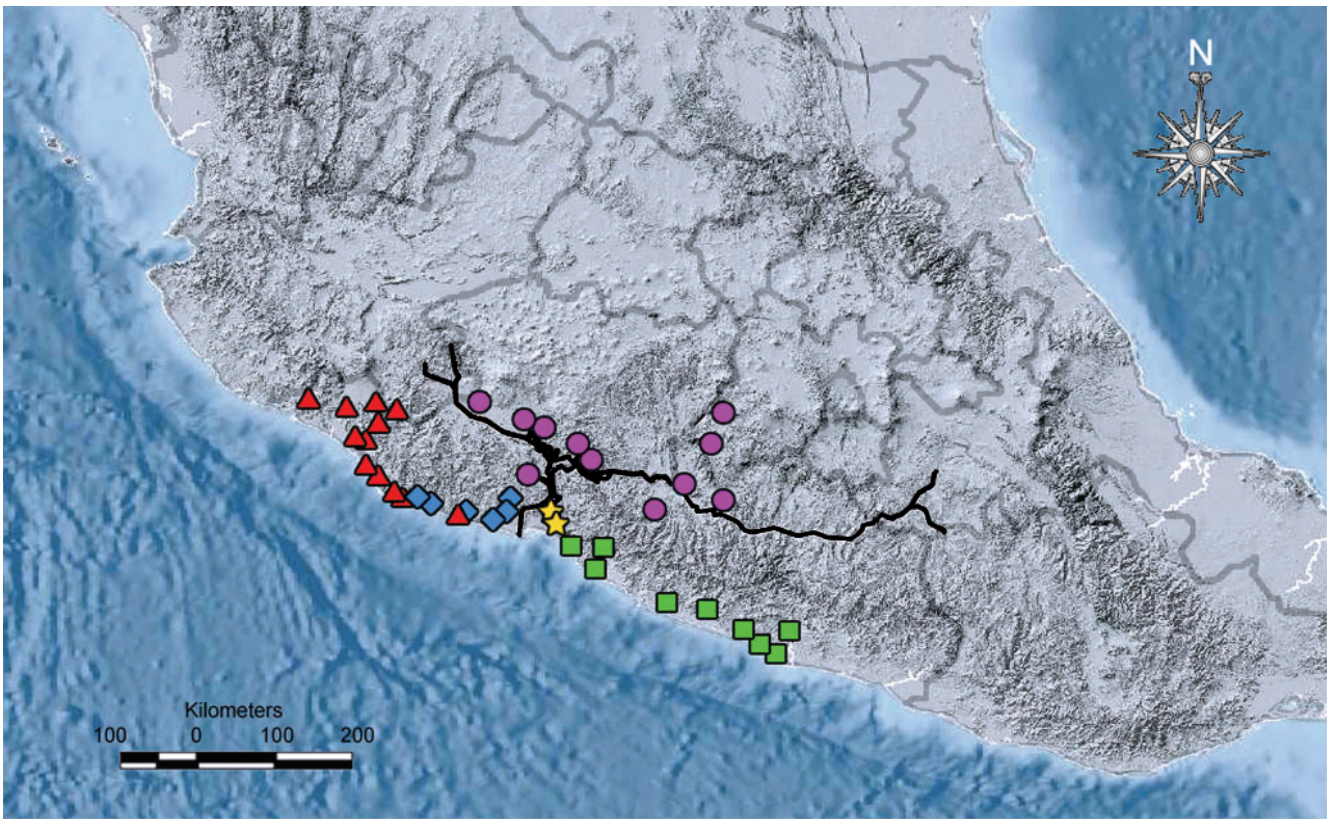

Fig. 62. Map showing records of *Brachypelma* Mexican red-knee, flame-knee and red-legged tarantulas in Colima, Guerrero and Michoacán states. Triangles, *B. hamorii*; squares, *B. smithi*; diamonds, *B. baumgarteni*; stars, *B. boehmei*; circles, *B. auratum*. The dark black line represents the Balsas River basin.

morphological judgments of species boundaries (Ortíz and Francke 2016). However, most taxonomists base their conclusions on a suite of complex morphological characters, rather than relying on part of a single gene (Will and Rubinoff 2004). While it is true that DNA-based methods are not demonstrably more objective, accurate or useful than morphology or other sources of phenotypic data for species identification (Prendini 2005), DNA barcoding is a very useful technique that, together with morphology, field observations and collection, allows for better definition and delimitation of species (Scotland *et al*. 2003; Slowik and Blagoev 2012; Hendrixson *et al*. 2015). Furthermore, in the particular case of tarantulas, molecular markers allow for the correct identification of juveniles and females, which are traded much more frequently than adult males. The use of non-destructive sampling techniques, such as the removal of a single leg and cauterisation of the wound, render this approach quite feasible (Longhorn *et al*. 2007; Hamilton *et al*. 2011; Hendrixson *et al*. 2013).

Our phylogenetic analyses of the COI sequences using parsimony and Bayesian inference corroborated the monophyly of *B. hamorii* and *B. smithi*, with *B. annitha* nested within *B. smithi*, and *B. hamorii* as sister species of all other red-legged *Brachypelma* (Figs 1, 2). This result confirmed the need to redefine the species that form the Mexican red-kneed tarantula group, based on morphological and molecular evidence. The other *Brachypelma* species from the Pacific coast of Mexico (*B. auratum*, *B. baumgarteni* and *B. boehmei*), which are geographically distributed between the *B. hamorii* and *B. smithi* populations, also present concordance with the topologies obtained with the phylogenetic analyses. Although we consider that the morphological evidence is good enough to justify the delimitation of *B. hamorii* and *B. smithi* as distinct species, with *B. annitha* as a junior synonym of the latter, the use of molecular characters of the barcoding gene COI has enabled us to provide a more robust dataset to support this conclusion. Most DNA-based theraphosid species delimitation studies have been primarily done with *Aphonopelma* Pocock, 1901 within the United States (Graham *et al*. 2015; Hamilton *et al*. 2011, 2014, 2016; Hendrixson *et al*. 2013, 2015; Wilson *et al*. 2013). Other DNA-based studies include the South American *Grammostola* Simon, 1892, with which taxonomy has been problematic due to the morphological homogeneity of its species (Montes de Oca *et al*. 2016), the poorly studied group *Bonnetina* Vol, 2000 (Ortíz and Francke 2016), and a single work on the CITES-protected genus *Brachypelma* Simon, 1891 using exuviae to obtain DNA (Petersen *et al*. 2007). These studies show strong differences between the current morphology-based taxonomy, and the evidence from molecular and ecological data: in *Grammostola* and *Bonnetina* there are species that are difficult to separate using only morphological characters, but by using molecular characters can be identified with more certainty (Ortíz and Francke 2016). Hamilton *et al*. (2016) mentions that

the limitations of mtDNA have been documented extensively; specifically, gene tree/species tree incongruence and the haploid, non-recombining nature of the molecule, with mtDNA representing only one particular genealogy out of all possible within a genome. However, Petersen *et al*. (2007) shows that although DNA barcodes do not capture the dynamic process of evolution nor reflect the precise interrelationships within a group, they can provide legislators within a framework when enacting protection laws. This could translate into greater success in prosecuting those involved in the illegal pet trade. It is agreed that mtDNA alone is insufficient for precise species delimitation; however, it can be useful for identification if the findings correspond with morphological evidence. In the present case, we support the use of molecular markers for identification of *Brachypelma* species.

With the taxonomic status now clear and concise delimitations set for the populations of Guerrero and of Jalisco, Colima and Michoacán, further protection strategies can now be implemented. The clear demarcation between the two species of Mexican red-kneed tarantulas has an important significance in helping to establish the correct identification of species that are illegally traded and that are difficult to identify at a glance by PROFEPA officials, who are responsible for the protection of fauna and flora in Mexico. The barcode marker COI for these tarantulas proved to be sufficient for correct species identification. Thus, it may be a useful tool for preventing black market trade and reintroducing tarantulas into the right distribution areas. Because of this, we are also creating a genetic library of Mexican tarantulas as part of the Wildlife Barcode Project in Mexico, to be used as a reference for the authorities responsible for species conservation.

Conservation issues

CITES is the most important international convention dealing with wildlife conservation. The fundamental concept behind CITES is to protect and control the international trade of organisms that may be threatened or endangered in any of the signatory countries (Schultz and Schultz 2009). However, despite increased recognition, these trade measures do not necessarily benefit wild species. Moreover, it is often difficult to assess the consequences of such measures as the criteria used to make listing decisions include little consideration (if any) of whether proposed trade measures will be effective (Hutton and Dickson 2000). While there have been numerous revisions to the listing criteria, they still focus almost exclusively on the biological and trade status of the species and scarcely touch on whether the listing will benefit the conservation status of the species (Dickinson 2002).

At sustainable levels of consumption, both wildlife and people benefit from trade. Granting people an economic stake in wildlife provides the best incentive for careful stewardship of species and habitats (Carey 1999). Nevertheless, wild populations of red-legged tarantulas are now declining. Habitat destruction combined with cultural bias against these spiders and a lack of economic interest in their conservation have led to the current practice of killing tarantulas that are found in fields or houses. Tarantulas are seen as harmful creatures in many local communities. One negative result of the *Brachypelma* CITES listing has been a decrease in the supply of some species, leading to increased desirability and thus demand. This has encouraged the development of a black market, which smuggles protected species both locally and abroad (Reichling 2003). A study on the concept of controlled harvesting in Mexico is necessary as there is currently no provision to enable sustainable exploitation of such a resource (López and Íñigo 2009). Unfortunately, over the past few years, at least 3000 specimens of Mexican tarantulas were reportedly sent to Europe or the United States; most were red-kneed tarantulas (PROFEPA, unpub. data).

Red-kneed tarantulas are among the ten most trafficked animal species in Mexico (PROFEPA 2009). They are collected for profit by people in need to sustain themselves and their families (Schultz and Schultz 2009). Unfortunately, collectors disturb the habitat and do not attempt to maintain sustainable harvesting practices. Traffickers pay the collectors around US$2–3 dollars per tarantula, which can be sold for up to US$200 dollars on the international market (Inecc 2012). Large tracts of land are pitted from excavation of burrows. Habitat is further lost during the rainy season due to landslides. The traffickers have unique methods of facilitating illicit traffic, often hiding tarantula specimens in photographic film containers, small plastic tubes or plastic bags (BWPM 2014). The animals are crammed against each other and many die due to dehydration, insufficient space during moulting or suffocation in their own exuviae (Rojo 2004). Sometimes the orange-red markings on the legs are covered up with black marker in an attempt to pass them off as non-protected species (R. West, personal communication).

Very little is known about the conservation status of Mexican *Brachypelma* species, especially those restricted to areas particularly vulnerable to overexploitation. In general, tarantulas tend to have clumped distributions in small areas with specific soil types, and are ‘common’ only sporadically across their entire geographic range. These factors leave them vulnerable to natural stochastic events (Reichling 2003). One of the authors observed this during the hurricane season of 2012–13, when the Mexican government reported serious environmental damage and changes to the flow of rivers along the Pacific coast. The coast of Guerrero was one of the most heavily affected areas, with extensive flooding of the Papagayo River nearly causing the complete destruction of two *B. smithi* populations.

Until a thorough assessment is undertaken of the environmental, legal, social and economic factors impacting on wildlife trade in Mexico, there is little that can be done to develop successful management strategies and species conservation initiatives. In addition, it is essential to explore other non-subtractive economic endeavours such as tourism, wildlife observation or sale of captive-bred animals to provide alternative incomes for local communities and to avoid further damage to wild populations. Legal breeders should also be included in the conservation strategies of Mexican red-kneed tarantulas to support their efforts to breed and reintegrate tarantulas in their natural distribution ranges.

Acknowledgements

This publication is a requirement of the PhD graduate training program of Jorge Mendoza at the Posgrado en Ciencias Biológicas of the Universidad Nacional Autónoma de México (UNAM). JM thanks the

Instituto de Biología (IBUNAM) and the Posgrado en Ciencia Biológicas of the UNAM for the program received. JM would also like to thank the Consejo Nacional de Ciencia y Tecnología (CONACYT) for providing financial support of his postgraduate studies as well as the grants required for a research stay at the Muséum National d'Histoire Naturelle in Paris, France (MNHNP), the Natural History Museum in London, United Kingdom (NHM) and the Senckenberg Naturmuseum in Frankfurt, Germany (SNMF). We thank Janet Beccaloni, Christine Rollard, Elise-Anne Leguin, Peter Jäger and Julia Altmann for providing access to the type and historical specimens. Stuart Longhorn and Ray Gabriel are thanked for their assistance and hospitality during JM's research stay in Europe. We thank Virginia Leon for her support to travel to Europe, Andrea Jiménez for her assistance during molecular work and Alejandro Oceguera for providing valuable comments on an earlier version of the manuscript. JM thanks the members of the laboratory of arachnology (CNAN) for their support and assistance on field trips. JM thanks R. Ramírez, J. Hinojosa, E. Hijmensen and E. Goyer for their assistance during field trips. Images of live specimens and habitat were kindly provided by Emmanuel Goyer and Guillermo Vila. We also thank Emmanuel Goyer for language revision and valuable comments. We also thank the editors and reviewers for their critical reading and valuable comments. The specimens were collected under scientific collection permit FAUT-0175, authorised by SEMARNAT for Oscar F. Francke. The present project was supported by MEXBOL of CONACYT (project 251085) and the Wildlife Barcode Project in Mexico, sponsored by Google's Global Impact Awards.

References

Arnedo, M., and Fernández, M. (2007). Mitochondrial markers reveal deep population subdivision in the European protected spider *Macrothele calpeiana* (Walckenaer, 1805) (Araneae, Hexathelidae). *Conservation Genetics* **8**, 1147–1162. doi:10.1007/s10592-006-9270-2

Barrett, R., and Hebert, P. (2005). Identifying spiders through DNA barcodes. *Canadian Journal of Zoology* **83**, 481–491. doi:10.1139/z05-024

Baxter, R. N. (1993). 'Keeping and Breeding Tarantulas.' (Chudleigh Publishing: Ilford, UK.)

Bertani, R. (2000). Male palpal bulbs and homologous features in Theraphosinae (Araneae, Theraphosidae). *The Journal of Arachnology* **28**, 29–42. doi:10.1636/0161-8202(2000)028[0029:MPBAHF]2.0.CO;2

Bertani, R. (2001). Revision, cladistic analysis and zoogeography of Vitalius, Nhandu and Proshapalopus, with notes on other theraphosine genera (Araneae, Theraphosidae). *Arquivos de Zoologia* **36**, 265–356.

Blagoev, G., Hebert, P., Adamowicz, S., and Robinson, E. (2009). Prospects for using DNA barcoding to identify spiders in species-rich genera. *ZooKeys* **16**, 27–46. doi:10.3897/zookeys.16.239

Blagoev, G. A., deWaard, J. R., Ratnasingham, S., deWaard, S. L., Lu, L., Robertson, J., Telfer, A. C., and Hebert, P. D. N. (2016). Untangling taxonomy: a DNA barcode reference library for Canadian spiders. *Molecular Ecology Resources* **16**, 325–341. doi:10.1111/1755-0998.12444

Bond, J. E., and Stockman, A. K. (2008). An integrative method for delimiting cohesion species: finding the population-species interface in a group of Californian trapdoor spiders with extreme genetic divergence and geographic structuring. *Systematic Biology* **57**, 628–646. doi:10.1080/10635150802302443

Briscoe, A. G., Goodacre, S., Masta, S. E., Taylor, M. I., Arnedo, M. A., Penney, D., Kenny, J., and Creer, S. (2013). Can long-range PCR be used to amplify genetically divergent mitochondrial genomes for comparative phylogenetics? A case study within spiders (Arthropoda : Araneae). *PLoS One* **8**, e62404. doi:10.1371/journal.pone.0062404

Brown, S. D. J., Collins, R. A., Boyer, S., Lefort, M. C., Malumbres-Olarte, J., Vink, C. J., and Cruickshank, R. H. (2012). SPIDER: an R package for the analysis of species identity and evolution, with particular reference to DNA barcoding. *Molecular Ecology Resources* **12**, 562–565. doi:10.1111/j.1755-0998.2011.03108.x

BWPM (2014). Códigos de Barras de la Vida Silvestre México. Available at http://bwp-mex.blogspot.mx/ [Accessed 12 December 2015].

Carey, J. E. (1999). Improving the efficacy of CITES by providing the proper incentives to protect endangered species. *Washington University Law Review* **77**, 1291–1322.

Chan, A., Chiang, L., Hapuarachchi, H., Tan, C., Pang, S., Lee, R., Lee, K., Ng, L., and Lam-Phua, S. (2014). DNA barcoding: complementing morphological identification of mosquito species in Singapore. *Parasites & Vectors* **7**, 569. doi:10.1186/s13071-014-0569-4

Chen, J., Li, Q., Kong, L., and Yu, H. (2011). How DNA barcodes complement taxonomy and explore species diversity: the case study of a poorly understood marine fauna. *PLoS One* **6**, e21326. doi:10.1371/journal.pone.0021326

Dickinson, B. (2002). International conservation treaties, poverty and development: the case of CITES. *Natural Resource Perspectives* **74**, 1–4.

Folmer, O., Black, M., Hoech, W., Lutz, R., and Vrijenhoeck, R. (1994). DNA primers for amplification of mitochondrial cytochrome *c* oxidase subunit I from diverse metazoan invertebrates. *Molecular Marine Biology and Biotechnology* **3**, 294–299.

Goloboff, P. A., Farris, J. S., and Nixon, K. C. (2008). TNT, a free program for phylogenetic analysis. *Cladistics* **24**, 774–786. doi:10.1111/j.1096-0031.2008.00217.x

Graham, M. R., Hendrixson, B. E., Hamilton, C. A., and Bond, J. E. (2015). Miocene extensional tectonics ex-plain ancient patterns of diversification among turret-building tarantulas (Aphonopelma mo-jave group) in the Mojave and Sonoran deserts. *Journal of Biogeography* **42**, 1052–1065.

Greenstone, M., Rowley, D., Heimbach, U., Lundgren, J., Pfannenstiel, R., and Rehner, S. (2005). Barcoding generalist predators by polymerase chain reaction: carabids and spiders. *Molecular Ecology* **14**, 3247–3266. doi:10.1111/j.1365-294X.2005.02628.x

Hamilton, C. A., Formanowicz, D. R., and Bond, J. E. (2011). Species delimitation and phylogeography of *Aphonopelma hentzi* (Araneae, Mygalomorphae, Theraphosidae): cryptic diversity in North American tarantulas. *PLoS One* **6**, e26207. doi:10.1371/journal.pone.0026207

Hamilton, C. A., Hendrixson, B. E., Brewer, M. S., and Bond, J. (2014). An evaluation of sampling effects on multiple DNA barcoding methods leads to an integrative approach for delimiting species: a case study of the North American tarantula genus *Aphonopelma* (Araneae, Mygalomorphae, Theraphosidae). *Molecular Phylogenetics and Evolution* **71**, 79–93. doi:10.1016/j.ympev.2013.11.007

Hamilton, C. A., Hendrixson, B. E., and Bond, J. E. (2016). Taxonomic revision of the tarantula genus *Aphonopelma* Pocock 1901 (Araneae, Mygalomorphae, Theraphosidae) within the United States. *ZooKeys* **560**, 1–340. doi:10.3897/zookeys.560.6264

Hancock, K. and Hancock, J. (1989). Sex Determination of Immature Theraphosid Spiders from Their Cast Skins.' (Published by the authors: Southminster, England.)

Hebert, P. D., Cywinska, A., Ball, S. L., and deWaard, J. R. (2003). Biological identifications through DNA barcodes. *Proceedings of the Royal Society of London. Series B, Biological Sciences* **270**, 313–321. doi:10.1098/rspb.2002.2218

Hendrixson, B. E., DeRussy, B. M., Hamilton, C. A., and Bond, J. E. (2013). An exploration of species boundaries in turret-building tarantulas of the Mojave Desert (Araneae, Mygalomorphae, Theraphosidae, Aphonopelma). *Molecular Phylogenetics and Evolution* **66**, 327–340. doi:10.1016/j.ympev.2012.10.004

Hendrixson, B. E., Guice, A. V., and Bond, J. E. (2015). Integrative species delimitation and conservation of tarantulas (Araneae, Mygalomorphae, Theraphosidae) from a North American biodiversity hotspot. *Insect Conservation and Diversity* **8**, 120–131. doi:10.1111/icad.12089

Huelsenbeck, J. P., and Ronquist, F. (2001). MRBAYES: Bayesian inference of phylogenetic trees. *Bioinformatics* **17**, 754–755. doi:10.1093/bioinformatics/17.8.754

Hutton, J., and Dickson, B. (2000). 'Endangered Species, Threatened Convention: the Past, Present and Future of CITES.' (Earthscan: London.)

Inecc (2012). Tráfico ilegal de especies silvestres y sus impactos. Available at http://www.inecc.gob.mx/descargas/dgioece/2012_sem_trafico_pon01_alow.pdf [Accessed 9 January 2016].

Katoh, K., Misawa, K., Kuma, K., and Miyata, T. (2002). MAFFT: a novel method for rapid multiple sequence alignment based on fast Fourier transform. *Nucleic Acids Research* **30**, 3059–3066. doi:10.1093/nar/gkf436

Katoh, K., Kuma, K., Toh, H., and Miyata, T. (2005). MAFFT version 5: improvement in accuracy of multiple sequence alignment. *Nucleic Acids Research* **33**, 511–518. doi:10.1093/nar/gki198

Kearse, M., Moir, R., Wilson, A., Stones-Havas, S., Cheung, M., Sturrock, S., Buxton, S., Cooper, A., Markowitz, S., Duran, C., Thierer, T., Ashton, B., Mentjies, P., and Drummond, A. (2012). Geneious Basic: an integrated and extendable desktop software platform for the organization and analysis of sequence data. *Bioinformatics* **28**, 1647–1649. doi:10.1093/bioinformatics/bts199

Kuntner, M., and Agnarsson, I. (2011). Biogeography and diversification of hermit spiders on Indian Ocean islands (Nephilidae : Nephilengys). *Molecular Phylogenetics and Evolution* **59**, 477–488. doi:10.1016/j.ympev.2011.02.002

Locht, A., Yáñez, M., and Vázquez, I. (1999). Distribution and natural history of Mexican species of *Brachypelma* and *Brachypelmides* (Theraphosidae, Theraphosinae) with morphological evidence for their synonymy. *The Journal of Arachnology* **27**, 196–200.

Longhorn, S., Nicholas, M., Chuter, J., and Vogler, A. (2007). The utility of molecular markers from non-lethal DNA samples of the CITES II protected 'tarantula' *Brachypelma vagans* (Araneae, Theraphosidae). *The Journal of Arachnology* **35**, 278–292. doi:10.1636/S05-62.1

López, X., and Íñigo, E. (2009). La captura de aves silvestres en México: una tradición milenaria y las estrategias para regularla. *Biodiversitas* **83**, 11–15.

Mendoza, J. I. M. (2014). Taxonomic revision of *Hemirrhagus* Simon, 1903 (Araneae: Theraphosidae, Theraphosinae), with description of five new species from Mexico. *Zoological Journal of the Linnean Society* **170**, 634–689. doi:10.1111/zoj.12112

Montes de Oca, L., D'Elía, G., and Pérez-Miles, F. (2016). An integrative approach for species delimitation in the spider genus *Grammostola* (Theraphosidae, Mygalomorphae). *Zoologica Scripta* **45**, 322–333. doi:10.1111/zsc.12152

Mundie, D. A. (1995). The NBS/ISCC Color System / David A. Mundie Pittsburgh, PA: Polymath Systems 535.6 dc-20. Available at http://www.anthus.com/Colors/NBS.html [Accessed 12 March 2015].

Ortíz, D., and Francke, F. (2016). Two DNA barcodes and morphology for multi-method species delimitation in *Bonnetina* tarantulas (Araneae : Theraphosidae). *Molecular Phylogenetics and Evolution* **101**, 176–193. doi:10.1016/j.ympev.2016.05.003

Pante, E., Schoelinck, C., and Puillandre, N. (2015). From integrative taxonomy to species description: one step beyond. *Systematic Biology* **64**, 152–160. doi:10.1093/sysbio/syu083

Pérez-Miles, F. (1989). Variaci6n relativa de caracteres somaticos y genitales en Grammostola mollicoma(Araneae, Theraphosidae). *Journal of Arachnology* **17**, 263–274.

Pérez-Miles, F. (1994). Tarsal scopula division in Theraphosinae (Araneae, Theraphosidae): its systematic significance. *The Journal of Arachnology* **22**, 46–53.

Peters, H. J. (2000). Tarantulas of the world. *Kleiner Atlas der Vogelspinnen* **1**, 148. (Published by the author.)

Peters, H. J. (2003). 'Tarantulas of the World: Amerika's Vogelspinnen.' (Published by the author: Wegberg, Germany.)

Petersen, F. T., Damgaard, J., and Meier, R. (2007). DNA taxonomy: how many DNA sequences are needed for solving a taxonomic problem? The case of two parapatric species of louse flies (Diptera : Hippoboscidae : Ornithomya Latreille, 1802). *Arthropod Systematics & Phylogeny* **65**, 119–125.

Pickard-Cambridge, F. O. (1897). Arachnida – Araneida and Opiliones. Biologia Centrali-Americana *Zoology (Jena, Germany)* **2**, 1–40.

Pocock, R. I. (1903). On some genera and species of South-American Avicula riidae. *Annals & Magazine of Natural History* **11**, 81–115. doi:10.1080/00222930308678729

Posada, D. (2008). jModelTest: phylogenetic model averaging. *Molecular Biology and Evolution* **25**, 1253–1256. doi:10.1093/molbev/msn083

Prendini, L. (2005). Comment on "identifying species through DNA barcodes". *Canadian Journal of Zoology* **83**, 498–504. doi:10.1139/z05-025

PROFEPA (2009). 'La Vida Silvestre y su Protección Legal.' (Secretaria del Medio Ambiente y Recursos Naturales: Mexico.)

Reichling, S. B. (2003). 'Tarantulas of Belize.' (Krieger Publishing Company: Malabar, FL.)

Rojo, R. (2004). Las Tarántulas de México: pequeños gigantes incomprendidos. *Biodiversitas* **56**, 7–11.

Ronquist, F., and Huelsenbeck, J. P. (2003). MRBAYES 3: Bayesian phylogenetic inference under mixed models. *Bioinformatics* **19**, 1572–1574. doi:10.1093/bioinformatics/btg180

Schmidt, G. (1992*a*). *Brachypelma* Simon 1890 oder *Euathlus* Ausserer 1875? (Araneida: Theraphosidae: Theraphosinae). *Arachnologischer Anzeiger* **3**, 9–11.

Schmidt, G. (1992*b*). *Brachypelma auratum* sp. n., die sogenannte Hochlandform von *Brachypelma smithi* (Araneida: Theraphosidae: Theraphosinae). *Arachnologischer Anzeiger* **3**, 9–14.

Schmidt, G. (1993). 'Vogelspinnen: Vorkommen, Lebensweise, Haltung und Zucht, mit Bestimmungsschlüsseln für Alle Gattungen, Vierte Auflage.' (Landbuch Verlag: Hannover, Germany.)

Schmidt, G. (1997). Bestimmungsschlüssel für die gattungen der unterfamilie Theraphosinae (Araneae : Theraphosidae). *Arachnologisches Magazin* **3**, 1–27.

Schmidt, G. (2003). Die Vogelspinnen: eine weltweite Übersicht. (Neue Brehm-Bücherei: Hohenwarsleben, Germany.)

Schultz, S. A., and Schultz, M. J. (2009). 'The Tarantula Keepers Guide.' (Barron's Educational Series: New York, NY.)

Scotland, R. W., Hughes, C., Bailey, D., and Wortley, A. (2003). The Big Machine and the much-maligned taxonomist. *Systematics and Biodiversity* **1**, 139–143. doi:10.1017/S1477200003001178

Simon, E. (1891). Liste des Aviculariides qui habitant le Mexique et l'Amérique centrale. *Actes de la Société Linnéenne de Bordeaux* **44**, 327–339.

Slowik, J., and Blagoev, G. A. (2012). A survey of spiders (Arachnida: Araneae) of Prince Wales Island, Alaska; combining morphological and DNA barcode identification techniques. *Insecta Mundi* **251**, 1–12.

Smith, A. M. (1994). 'Tarantula Spiders Tarantulas of the USA and Mexico.' (Fitzgerald: London.)

Sun, Y., Li, Q., Kong, L., and Zheng, X. (2012). DNA barcoding of Caenogastropoda along coast of China based on the COI gene. *Molecular Ecology Resources* **12**, 209–218. doi:10.1111/j.1755-0998.2011.03085.x

Tesmoingt, M., Cleton, F., and Verdez, J. M. (1997*a*). Description de *Brachypelma annitha* n. sp. et de *Brachypelma hamorii* n. sp. mâles et femelles, nouvelles espèces proches de *Brachypelma smithi* (Cambridge, 1897) du Mexique. *Arachnides* **32**, 8–20.

Tesmoingt, M., Cleton, F., and Verdez, J. M. (1997*b*). Description de *Brachypelma annitha* n. sp. et de *Brachypelma hamorii* n. sp. mâles et femelles, nouvelles espèces proches de *Brachypelma smithi* (Cambridge, 1897) du Mexique. 2ème partie. *Arachnides* **33**, 2–10.

Teyssié, F. (2015). 'Tarantulas of the World.' (NAP Editions: France.)

West, R. C. (2005). The *Brachypelma* of Mexico. *Journal of the British Tarantula Society* **20**, 108–119.

Will, K., and Rubinoff, D. (2004). Myth of the molecule: DNA barcodes for species cannot replace morphology for identification and classification. *Cladistics* **20**, 47–55. doi:10.1111/j.1096-0031.2003.00008.x

Wilson, J. S., Gunnell, C. F., Wahl, D. B., and Pitts, J. P. (2013). Testing the species limits of the tarantulas (Araneae: Theraphosidae) endemic to California's Southern Coast Ranges, USA. *Insect Conservation and Diversity* **6**, 365–371.

World Spider Catalog (2016). Version 17. Natural History Museum Bern. Available at http://wsc.nmbe.ch [Accessed 25 January 2016].

Handling editor: Mark Harvey

Appendix 1. Terminal taxa, specimens and tissue samples used for phylogenetic analyses of seven species in the genus *Brachypelma*

Material examined is deposited in the Colección Nacional de Arácnidos (CNAN), Instituto de Biología, Universidad Nacional Autónoma de México, Mexico City

Outgroup

Two theraphosid sequences were retrieved from GenBank for cladistic analyses: *Psalmopoeus cambridgei* Pocock, 1895 447_SC_AB (JQ412455) and *Eupalaestrus campestratus* (Simon, 1891) 446_SC_AB (JQ412446). Both specimens are deposited in the Bangor University collection, United Kingdom.

Ingroup

1. *Brachypelma albiceps* (Pocock, 1903): 1 ♂ (CNAN-Ar003412), MEXICO: Guerrero, Mpio. Copalillo, 14.X.2008, coll. J. Mendoza. 1 juv. ♀ (CNAN-Ar007839), MEXICO: Guerrero, Mpio. Tixtla de Guerrero, 23.IX.2012, coll. J. Mendoza, G. Contreras, J. Lopez, D. Ortiz. 1 juv. ♀ (CNAN-Ar007850), MEXICO: Guerrero, Mpio. Azoyu, VII.2011, coll. A. Alcaraz.
2. *Brachypelma auratum* Schmidt, 1992: 1 ♂ (CNAN-Ar003658), MEXICO: Michoacán, Mpio. Los Reyes, 02.II.2013, coll. J. Mendoza, G. Contreras, D. Ortiz, D. Barrales. 1 juv. ♀ (CNAN-Ar007136), MEXICO: Guerrero, Mpio. Arcelia, 03.II.2013, coll. J. Mendoza, G. Contreras, J. Cruz, D. Ortiz. 1 juv. ♀ (CNAN-Ar007164), MEXICO: Michoacán, Mpio. San Lucas, 02.II.2013, coll. J. Mendoza, G. Contreras, D. Ortiz, D. Barrales.
3. *Brachypelma baumgarteni* Smith, 1993: 1 ♀ (CNAN-Ar007151), MEXICO: Michoacán, Mpio. Lázaro Cárdenas, 10.XII.2013, coll. J. Mendoza. 1 juv. ♀ (CNAN-Ar007161), MEXICO: Michoacán, Mpio. Lázaro Cárdenas, Carr. Neixpa-Manzanillo, 11.XII.2013, coll. J. Mendoza. 1 subad. ♂ (CNAN-Ar007835), MEXICO: Michoacán, Mpio. Lázaro Cárdenas, 11.XII.2013, coll. J. Mendoza.
4. *Brachypelma boehmei* Schmidt & Klaas, 1993: 1 ♀ (CNAN-Ar007185), MEXICO: Guerrero, Mpio. La Unión de Isidoro Montes de Oca, 12.XII.2013, coll. J. Mendoza. 1 ♀ (CNAN-Ar007186), MEXICO: Guerrero, Mpio. La Unión de Isidoro Montes de Oca, 12.XII.2013, coll. J. Mendoza. 1 ♂ (CNAN-Ar007833), MEXICO: Guerrero, Mpio. La Unión de Isidoro Montes de Oca, 12.XII.2013, coll. J. Mendoza.
5. *Brachypelma hamorii* Tesmoingt, Cleton & Verdez, 1997: 1 ♂ (CNAN-Ar003614), MEXICO: Colima, Mpio. Tecomán, 01.XII.2012, coll. E. Goyer, E. Hijmensen, D. Ortiz. 2 ♂ (CNAN-Ar007163, CNAN-Ar007826), MEXICO: Colima, Mpio. Tecomán, 05.XII.2013, coll. D. Ortiz, D. Barrales, G. Contreras. 1 ♂ (CNAN-Ar007168), MEXICO: Colima, Mpio. Tecomán, 03.XII.2013, coll. D. Ortiz, D. Barrales, G. Contreras. 1 ♂ (CNAN-Ar007827), MEXICO: Colima, Mpio. Colima, 03.XII.2013, coll. D. Ortiz, D. Barrales, G. Contreras. 1 ♂ (CNAN-T0900), MEXICO: Colima, Mpio. Tecomán, 05.XII.2013, coll. D. Ortiz, D. Barrales, G. Contreras.
6. *Brachypelma klaasi* (Schmidt & Krause, 1994): 1 ♂ (CNAN-Ar007160), MEXICO: Jalisco, Mpio. Cihuatlán, 04.XII.2013, coll. D. Ortiz, D. Barrales, G. Contreras. 1 ♂ (CNAN-Ar007162), MEXICO: Colima, Mpio. Manzanillo, 04.XII.2013, coll. D. Ortiz, D. Barrales, G. Contreras.
7. *Brachypelma smithi* (F. O. Pickard-Cambridge, 1897): 1 ♀ (CNAN-Ar004131), MEXICO: Guerrero, Mpio. Acapulco, collection of J. Mendoza. 1 juv. ♂ (CNAN-Ar007140), MEXICO: Guerrero, Mpio. Acapulco, 20.IX.2012, coll. J. Mendoza, G. Contreras, J. Cruz, D. Ortiz. 2 ♀ (CNAN-Ar007143, CNAN-Ar007144) and 1 ♂ CNAN-Ar007832, MEXICO: Guerrero, Mpio. Acapulco, 13.XII.2013, coll. J. Mendoza. 1 ♀ (CNAN-Ar003611), MEXICO: Guerrero, Mpio. Acapulco, collection of J. Mendoza (pet trade labelled as *B. annitha*).